Nonmammalian gonadotropin-releasing hormone molecules in the brain of promoter transgenic rats

Ishwar S. Parhar*†, Tomoko Soga*, Satoshi Ogawa*, Sonoko Ogawa‡, Donald W. Pfaff‡, and Yasuo Sakuma*

*Department of Physiology, Nippon Medical School, Tokyo 113-8602, Japan; and ‡Department of Neurobiology and Behavior, The Rockefeller University, New York, NY 10021

Contributed by Donald W. Pfaff, March 6, 2005

Mammalian gonadotropin-releasing hormone (GnRH1) and nonmammalian immunoreactive GnRH subtypes were examined in transgenic rats carrying an enhanced GFP (EGFP) reporter gene driven by a rat GnRH1 promoter. Double-label immunocytochemistry was performed on EGFP$^+$/GnRH1 brain sections by using antisera against GnRH1, GnRH2 (chicken II), GnRH3 (salmon), or seabream GnRH. EGFP$^+$/GnRH1 neurons were in the septal–preoptic hypothalamus but not in the midbrain, consistent with GnRH1-immunopositive neurons in WT rats. Apparent coexpression of EGFP$^+$/GnRH1 with other GnRH subtypes was observed. All EGFP$^+$ neurons in the septal–preoptic hypothalamus were GnRH1-immunopositive. However, only ≈80% of GnRH1-immunopositive neurons were EGFP$^+$, which awaits further elucidation. GnRH subtypes-immunopositive fibers and EGFP$^+$/GnRH1 fibers were conspicuous in the organum vasculosum of the lamina terminalis, median eminence, and surrounding the ependymal walls of the third ventricle and the aqueduct in the midbrain. These results demonstrate that the expression of the EGFP–GnRH1 transgene is restricted to the bona fide GnRH1 population and provide clear morphological evidence supporting the existence of GnRH1 neuronal subpopulations in the septal–preoptic hypothalamus, which might be driven by different segments of the GnRH promoter. This genetic construct permits analyses of promoter usage in GnRH neurons, and our histochemical approaches open questions about functional relations among isoforms of this peptide, which regulates reproductive physiology in its behavioral and endocrine aspects.

luteinizing hormone-releasing hormone | double-label immunocytochemistry | green fluorescent protein | hypothalamus | preoptic area

Until recently, the widely held view was that mammalian gonadotropin-releasing hormone (GnRH1), a decapeptide essential for reproduction and reproductive behavior in vertebrates, is the sole GnRH in the forebrain of mammals (1). However, from morphological, physiological, and evolutionary perspectives there is compelling evidence of distinct subpopulations of GnRH neurons in the mammalian forebrain. For example, retrograde tracer studies (2–6) and computerized 3D reconstruction (7) reveal distinct GnRH subsets within the forebrain GnRH neuronal population in rodents. Furthermore, new populations of GnRH neurons have been reported in the forebrain of rodents and primates whose developmental origin is different (8, 9) from the well documented placodal origin of GnRH1 neurons (10). Also, under certain physiological circumstances only a subpopulation of preoptic GnRH neurons expresses c-Fos protein, receptors for *N*-methyl-D-aspartate, galanin, or steroid hormones (11, 12). Furthermore, from an evolutionary perspective, it has become increasingly clear that some nonmammalian and mammalian vertebrates possess two or more GnRH subtypes in the brain (13–15), which include in addition to GnRH1, chicken II GnRH2 and salmon GnRH3 in rodents (16, 17). The cloning of GnRH receptor subtypes from the brains of several vertebrate species has further increased the likelihood that more than one molecular form of GnRH is present in the mammalian brain and that GnRH subtypes have multiple functions in addition to stimulating the release of gonadotropins (15, 18) and promoting sexual behavior (19, 20). Taken together, these studies emphasize the possibility that in the forebrain of mammals there exist GnRH populations functionally distinct from the originally discovered GnRH1.

Over the last decade, 16 structurally distinct GnRH forms have been isolated from different vertebrate species (15), and antisera against each GnRH subtype are readily available, which prompted us to investigate the possibility that more than one GnRH subtype can be expressed in different clonal neuronal populations in the rat brain. Transgenic rats carrying an EGFP reporter gene driven by a rat GnRH1 promoter were generated by Masakatsu Kato in our laboratory at Nippon Medical School (21), which we used for double-labeling studies with a variety of GnRH antisera. We compared these with the brain of WT rats immunoreacted with a battery of GnRH antisera specific for GnRH subtypes (mammalian GnRH1, chicken II GnRH2, salmon GnRH3, and seabream GnRH; see *Materials and Methods*).

Materials and Methods

WT and Transgenic Animals. Transgenic Wistar rats carrying an EGFP (Clontech) reporter gene, driven by 3.0 kb of rat GnRH1 promoter, were generated in our laboratory at Nippon Medical School (for details see ref. 21). The generation and use of transgenic rats were in accordance with the guidelines and approval of the Nippon Medical School Institutional Animal Care and Use Committee. WT and transgenic rats were housed under controlled conditions of temperature (24–26°C) and illumination (lights on 0800–2000 hours) with access to food and water ad libitium.

GnRH Antibodies. Several different GnRH antisera raised by different laboratories were used in the present study. Polyclonal rabbit antibodies specific for mammalian GnRH1 (635.5, gift from L. Jennes, University of Kentucky, Lexington; AB 1567, Chemicon); and monoclonal mouse anti-GnRH1 (LRH13, gift from K. Wakabayashi, Gunma University, Maebashi, Japan) were used. Polyclonal rabbit antibodies specific for GnRH2 (chicken II GnRH,1458, gift from J. King, University of Cape Town, Cape Town, South Africa; aCII6, gift from K. Okuzawa, National Research Institute of Aquaculture, Mie, Japan; ISP-II, supplied by I.S.P.); GnRH3 (salmon GnRH, lot 2, a gift from K. Aida, University of Tokyo, Tokyo; GF 6, a gift from N. Sherwood, University of Victoria, Victoria, Canada), and seabream GnRH (ISP 1, supplied by I.S.P.) also were used. The crossreactivities of GnRH1, GnRH2, GnRH3, and seabream GnRH antisera with various synthetic peptides have been determined by

Freely available online through the PNAS open access option.

Abbreviations: Aq, aqueduct; GnRH, gonadotropin-releasing hormone; HB, habenula; ME, median eminence; MM, mammillary body; MPOA, medial and median preoptic area; OVLT, organum vasculosum of the lamina terminalis; TT, tenia tecta.

†To whom correspondence should be addressed. E-mail: ishwar@nms.ac.jp.

© 2005 by The National Academy of Sciences of the USA

www.pnas.org/cgi/doi/10.1073/pnas.0501832102

Table 1. Distribution of GnRH subtype immunopositive neurons in the brain of WT and EGFP$^+$/GnRH1 and double-label GnRH neurons in transgenic rats

GnRH antibody	Antibody Concentration	Code	%CR with GnRH1	TT-SHi	MS-DB	MPOA	LS	OVLT	ME	Pe	SO	Soma/fibers VMHvL	Am	HB	PVP	CA1	MM	CG	IP	Septal–preoptic hypothalamus IR cells	IF cells	EGFP$^+$ cells	DL cells	% DL
GnRH1-EGFP[1]	—	—	—	+/+	+/+	+/+	−/+	−/+	−/+	+/+	+/+	+/+	−/+	+/+	−/+	−/+	+/+	−/+	−/+	—	—	901 ± 25	—	—
GnRH1	1:2,500	LRH13	100	+/+	+/+	+/+	−/−	−/+	−/+	+/+	+/+	+/+	−/+	−/+	−/+	−/+	−/+	−/+	−/+	962 ± 26	1044 ± 51	908 ± 49	860 ± 42	82 ± 1
GnRH1	1:8,000	635.5	NA	+/+	+/+	+/+	−/−	−/+	−/+	+/+	−/+	−/+	−/+	−/+	−/+	−/+	−/+	−/+	−/+	964 ± 88				
GnRH1	1:2,000	AB1567	100	−/+	+/+	+/+	−/−	−/+	−/+	−/−	−/+	−/+	−/+	−/+	−/+	−/+	−/+	−/+	−/+	124 ± 28				
GnRH2	1:4,000	aCII6	0.01	−/−	+/+	+/+	−/+	−/+	−/+	−/+	−/+	−/−	+/+	−/+	−/+	−/+	−/−	−/+	−/+	456 ± 84	413 ± 74	861 ± 41	288 ± 82	70 ± 2
GnRH2	1:3,000	1458	2.5	+/+	+/+	+/+	−/−	−/+	−/+	+/+	+/+	−/+	−/+	−/+	−/+	−/+	−/−	−/+	−/+	472 ± 8				
GnRH2	1:3,000	ISP II	NA	−/−	−/−	+/+	−/−	−/+	−/+	−/−	−/−	−/−	−/−	−/−	−/−	−/−	−/−	−/−	−/−	84 ± 20				
GnRH3	1:11,500	Lot. 2	0.01	+/+	+/+	+/+	−/−	−/+	−/+	−/+	+/+	+/+	−/+	−/+	−/+	−/+	−/−	−/+	−/+	516 ± 80	670 ± 76	972 ± 52	406 ± 24	60 ± 7
GnRH3	1:3,500	GF6	100	+/+	+/+	+/+	−/−	−/+	−/+	+/+	+/+	+/+	−/+	−/+	−/+	−/+	−/−	−/+	−/+	616 ± 18				
Seabream	1:5,000	ISP1	0.01	−/−	+/+	+/+	−/−	−/+	−/+	−/−	−/+	−/+	−/+	−/+	−/+	−/+	−/−	−/+	−/+	45 ± 8				

CR, cross reactivity; Shi, septohippocampal nucleus; MS-DB, medial septum/diagonal band of Broca; LS, lateral septum; Pe, periventricular hypothalamic nucleus; SO, supraoptic nucleus; VMHvl, ventrolateral part of ventromedial hypothalamus; Am, medial amygdaloid nucleus; PVP, periventricular thalamic nucleus; CA1, CA1 field of the hippocampus; CG, midbrain central gray; IP, interpeduncular nucleus; IR, peroxidase immunoreactivity; IF, immunofluorescence; DL, double-label; NA, not available. % DL, DL/IF × 100. +/− indicates presence/absence of cell soma (*Left*) and fibers (*Right*). GnRH immunoreactive and EGFP$^+$ cell numbers are mean ± SEM from three to four animals per antibody and four EGFP$^+$ animals. The sources (represented by code) of the antisera are given in *Materials and Methods*.

Fig. 1. Gel showing expression of EGFP amplicons. EGFP$^+$/GnRH1 rats show a 1,057-bp PCR amplicon in lanes 1, 3, 5, 8, 9, and 10, and EGFP$^-$ littermates in lanes 2, 4, 6, and 7. DNA size marker (M) in base pairs, is given.

RIA and expressed as percentage crossreactivity with mammalian GnRH1 (for details of crossreactivities see refs. 8 and 22–24; Table 1).

Peroxidase-Based Immunocytochemistry in WT Rats. Wistar rats (adult females, $n = 12$; adult males, $n = 3$) weighing 150–200 g were anesthetized with sodium pentobarbital (Nembutal, 35 mg/kg of body weight; Abbott). A single injection of colchicine (10 μg/5 μl) was placed stereotaxically into the lateral ventricle. The next day, the animals were anesthetized with an overdose of Nembutal and transcardially perfused with 200 ml of ice-cold PBS followed by 200 ml of 4% paraformaldehyde dissolved in 0.01 M phosphate buffer (PB; pH 7.5). The brains were removed, postfixed overnight in the same fixative, and cryoprotected in 20% sucrose in PB at 4°C overnight.

Coronal brain cryostat sections (30 μm thick) from Bregma +1.70 to −6.30 (25) were placed sequentially into one of three vessels, incubated in one of the polyclonal primary antiserum against GnRH subtypes (see Table 1), and processed for free-floating immunocytochemistry following a protocol modified from Parhar *et al.* (26). In brief, after incubation in primary antiserum, sections were incubated in biotinylated anti-rabbit IgG or anti-mouse IgG and avidin-biotinylated horseradish peroxidase complex (Vectastain ABC Elite kit, Vector Laboratories) and reacted with 0.05% 3,3′-diaminobenzidine tetrahydrochloride (Sigma) used as chromogen. Sections were then mounted onto slides, dehydrated, and cleared in xylene, and coverslips were applied with Permount (Fisher). Immunoreactivity was observed with the aid of an Olympus microscope.

Controls for Immunocytochemistry. Wistar rats (adult females, $n = 2$; adult males, $n = 5$) weighing 200–250 g were used as controls. To demonstrate the specificity of the primary antisera to GnRH, adjacent brain sections were incubated with primary antiserum preabsorbed with heterologous or its homologous GnRH peptide at concentrations ranging from 1 to 8 μg/ml of the primary antiserum at its working dilution overnight before use (see Table 1). BSA was added to preabsorb anti-BSA. Additional negative controls included omission of one of the primary antisera from the immunostaining protocol, to further eliminate possible nonspecific reaction.

Identification of Transgenic Rats. Transgenic rats ($n = 9$, 8–12 weeks old) carrying the EGFP–GnRH1 reporter gene were identified by PCR analysis of genomic DNA isolated from ear biopsies by using a Puregene DNA isolation kit (Gentra Systems). PCR was performed by using a thermal cycler (PerkinElmer GeneAmp PCR system 9700, Applied Biosystems). The final amplification mix (Applied Biosystems) included the sense primer (F2: 3′-TAC TAT GGT CTA CGC TGC ACT-5′, rGnRH1 promoter base pairs 3017–3037), antisense primer (ERI: 5′-ACT TGA AGA AGT CGT GCT GCT-3′, pEGFP-1 base pairs 335–355) specific for EGFP-coding sequences, and 20 ng of genomic DNA to amplify a 1,015-bp fragment of the GFP gene. Following the standard PCR conditions, each PCR product was analyzed on 1% agarose gel containing ethidium bromide and photographed with a gel

PHYSIOLOGY

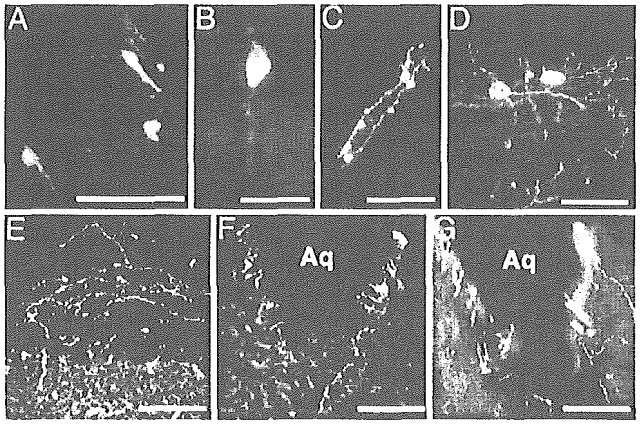

Fig. 2. Distribution of GnRH soma and fibers in the brain of EGFP$^+$/GnRH1 rats is shown. (*A*) TT. (*B* and *C*) Soma (*B*) and fibers (*C*) in the HB. (*D* and *E*) Soma (*D*) and fibers (*E*) in the MM. (*F* and *G*) EGFP$^+$/GnRH1 fibers (*F*) and Cy3-labeled GnRH2 fibers (*G*) surrounding the Aq in the midbrain. (Scale bars: *A* and *D–G*, 100 μm; *B* and *C*, 50 μm.)

visualization system (Electronic UV Transilluminator, UltraLum, Claremont, CA) (Fig. 1).

Double-Label Immunofluorescence in Transgenic Rats. Under Nembutal anesthesia (35 mg/kg of body weight), EGFP$^-$/GnRH1 rats (males, $n = 2$; females, $n = 7$) received a single stereotaxic injection of colchicine (10 μl/5 μl) into the lateral ventricle. The next day, animals were killed, and the brains were processed as in peroxidase-based immunocytochemistry (see above).

Coronal brain cryostat sections (30 μm thick) from Bregma +1.70 to −6.30 (25) were visualized for EGFP$^+$/GnRH1 neurons, and then incubated overnight at room temperature with antisera to GnRH1 (LRH13), GnRH2 (aCI16), or GnRH3 (lot 2). These antisera were used at a dilution of 1,500–2,000 with 0.01 M PBS (pH 7.6). After washes, sections were placed in Cy3 goat-anti-rabbit IgG (1:400 in PBS) or anti-mouse IgG for 2 h at room temperature and then mounted onto slides, and coverslips were applied with Vectashield (Vector Laboratories). Sections were viewed under a fluorescent microscope (DM RXA2, Leica Microsystems, Wetzlar, Germany) by using Texas red filter to reveal GnRH cells labeled with Cy3 (red fluorescence; Research Organics, Cleveland) and fluorescein-isothiocyanate filter to reveal the EGFP$^+$/GnRH1 neurons (green fluorescence). Digital images were captured on an Image Analysis System (Q5501W, Leica Microsystems) and superimposed for the observation of double-labeled cells. With PHOTOSHOP 4.0 (Adobe Systems, Seattle) the images were arranged into plates.

Cell Counts. In each brain three different GnRH antisera were applied to every third 30-μm section made from Bregma +1.70 to −6.30. The total number of GnRH-immunoreactive neurons in WT, EGFP$^-$/GnRH1, and double-labeled neurons in transgenic animals was counted in every third section spanning the septal–preoptic hypothalamus (Bregma +1.70 to −1.80). These counts were averaged across animals to determine mean ± SEM values for GnRH-immunopositive, EGFP$^-$/GnRH1, and double-labeled cell populations per individual brain (Table 1). All GnRH cells cut through the plane of the nucleus were counted in each section. Because the diameter of the GnRH cell nucleus is considerably smaller than the thickness of each cryostat section, no correction for double counting of cells was made.

Results

EGFP$^+$/GnRH1 neurons were observed in the tenia tecta (TT), septal–preoptic hypothalamus (septohippocampal nucleus, diagonal band of Broca, medial septum, medial preoptic area, retrochiasmatic supraoptic nucleus, ventrolateral part of the ventromedial hypothalamus), consistent with GnRH1-immunopositive cells in WT rats (Table 1). GnRH expression was not observed in the tectum of our adult rats, which is reported to be transiently expressed only during early development (9, 27).

Peroxidase-Based Immunocytochemistry in WT Rats. In the septal–preoptic hypothalamus, cells immunopositive for GnRH1 were more numerous than GnRH3 > GnRH2 > seabream GnRH (Table 1); these cells were fusiform in shape. GnRH cells were not segregated into nuclear clusters, instead they appeared as a loose continuum, which stretched from the TT to the septal–preoptic hypothalamus (Table 1).

Fibers immunoreactive to GnRH1, GnRH2, and GnRH3 were detected in the medial regions of the anterior olfactory nucleus, TT, septal–preoptic area, bed nucleus of the stria terminalis,

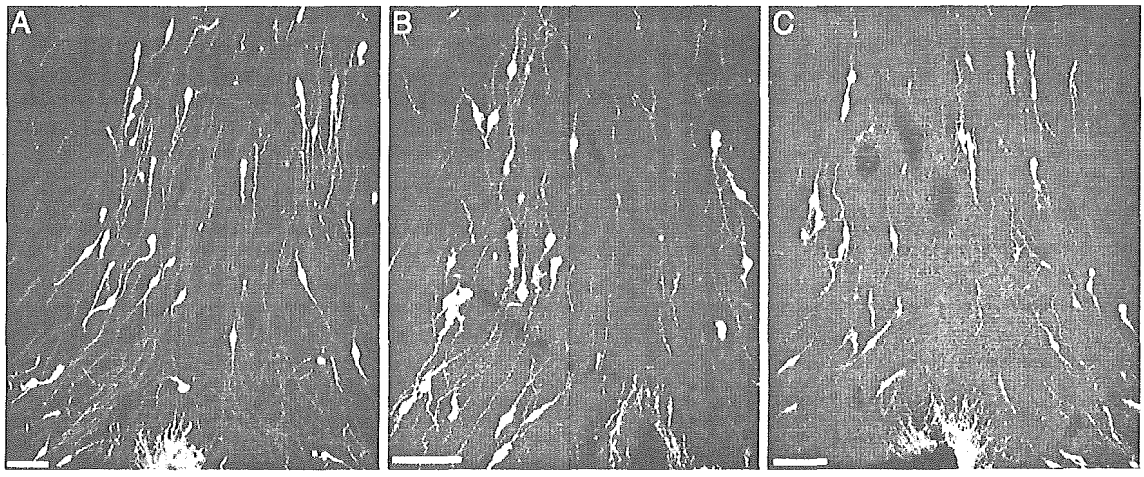

Fig. 3. Coronal sections through the caudal region of the septal–preoptic area of EGFP$^-$/GnRH1 rats immunoreactive to GnRH subtypes are shown. Cy3-labeled soma and fibers (red) reveal GnRH1 (LRH13) (*A*), GnRH3 (lot 2) (*B*), and GnRH2 (aCII6) (*C*). Note the typical fusiform shape of GnRH neurons and the abundance of EGFP$^+$ cells immunoreactive to GnRH1 in *A*; EGFP$^+$ soma and fibers coexpressing each GnRH subtype appear in yellow. Cy3-labeled nonmammalian GnRH soma and fibers (red) intermingled with EGFP$^+$/GnRH1 cells (green). (Scale bars, 50 μm.)

periventricular hypothalamic nucleus, medial amygdaloid nucleus, and medial mammillary body (MM), and along the ventral border of the interpeduncular nucleus (Table 1). GnRH fibers were consistently seen to course beneath the ependymal walls of the third ventricle and the aqueduct (Aq) in the midbrain central gray. However, the most conspicuous GnRH fibers were seen in the organum vasculosum of the lamina terminalis (OVLT) and the median eminence (ME) (Table 1).

No differences were detected between males and females when using any of the GnRH antisera. Immunostaining with seabream GnRH antisera was very weak. In control experiments, in which the GnRH antisera were preabsorbed with their respective homologous antigen or omitted from the procedure, no staining was evident in any of the sections. GnRH antisera preabsorbed with heterologous peptides did not abolish immunostaining.

Double-Label Immunofluorescence in Transgenic Rats. $EGFP^+$/GnRH1 cells were distributed as a loose continuum, which stretched from the TT to the septal–preoptic hypothalamus (Table 1 and Figs. 2 and 3). In the septal–preoptic hypothalamus, the number of $EGFP^+$/GnRH1 cells immunoreactive to antisera against GnRH subtypes varied in the following order: GnRH1 > GnRH3 > GnRH2. Double-label immunofluorescence, undertaken on brain sections from transgenic rats, revealed that ≈80% of GnRH1-immunopositive cells were $EGFP^-$ (Table 1 and Fig. 3*A*). Despite colocalization, cells immunoreactive to various GnRH antisera were seen scattered among $EGFP^+$/GnRH1 cells in the septal–preoptic hypothalamus (Fig. 3). $EGFP^+$/GnRH1 cells observed in the habenula (HB) and the MM were not immunoreactive to antisera against any of the GnRH subtypes (Fig. 2 *B* and *D*), whereas cells in the red nucleus were autofluorescent (data not shown).

$EGFP^+$/GnRH1 fibers were seen in the TT, septal–preoptic hypothalamus, HB, and the medial MM (Table 1 and Fig. 2 *C* and *E*). Fibers were consistently observed in the OVLT and ME, beneath the ependymal walls of the third ventricle, and in the Aq in the midbrain central gray (Figs. 2 *F* and *G*, 3, and 4 *A* and *B*). $EGFP^+$/GnRH1-, GnRH1-, GnRH2-, and GnRH3-immunopositive fibers were seen in close apposition or double-labeled in the lateral regions of the ME (Fig. 4 *A* and *B*) and in close apposition to $EGFP^+$/GnRH1 cell soma and fibers in the septal–preoptic hypothalamus (Figs. 3 and 4*C*).

Discussion

$EGFP^+$ neurons were detected in the TT, septal–preoptic hypothalamus, OVLT, and the ME, regions known to contain immunoreactive GnRH neurons and fibers in the rat brain (1) and in the TT of the Syrian hamster (28) and the musk shrew (29). Double-label studies confirmed that all $EGFP^+$ soma and terminal segments of axons were GnRH1-immunopositive (94%) but not all GnRH1-immunopositive cells were $EGFP^+$ (82%), which suggests the existence of GnRH neuronal subpopulations. In addition, it shows GnRH1 antiserum (LRH13) recognizes the precursor and the mature peptide indiscriminately (22), but differences in the availability of the absolute concentration of antigen along the axon preterminals, caused by rates of transport and/or sites of processing of the precursor, results in differences in double-labeling in preterminals versus terminal segments of axons in the OVLT and ME. Our results also demonstrate that the EGFP reporter gene driven by a rat GnRH1 promoter is more efficient for targeted expression of the reporter gene to GnRH-expressing neurons of the septal–preoptic hypothalamus compared with other reporter genes (e.g., *luc* and *lacZ*) driven by the human or murine GnRH promoters, which fail to provide GnRH neuron-restricted expression in transgenic mice (30).

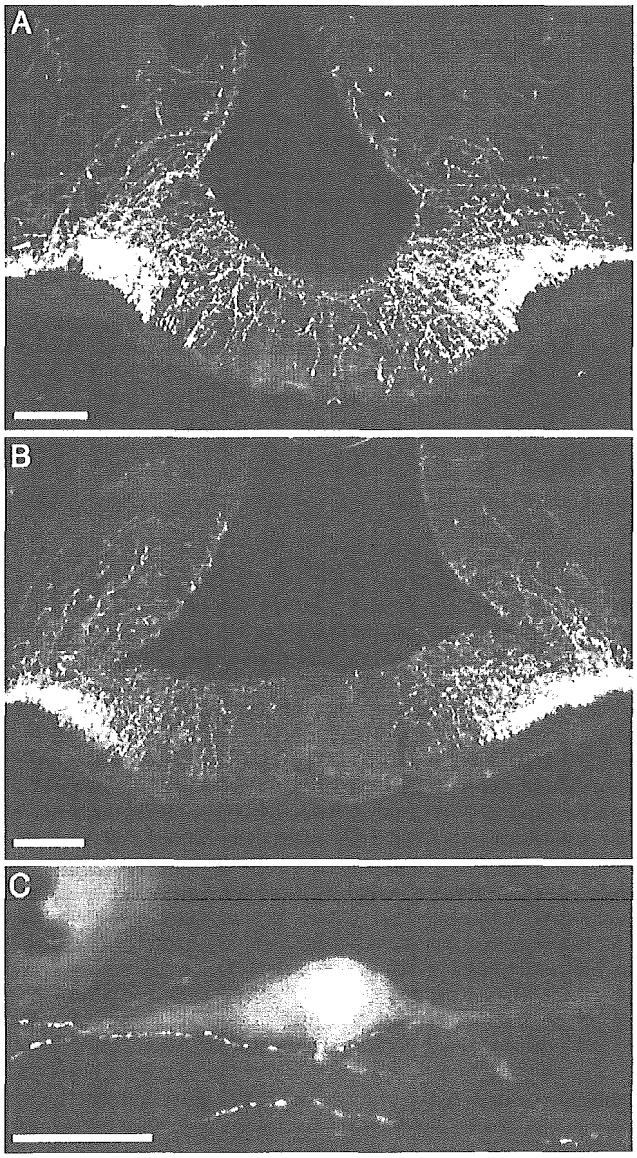

Fig. 4. Coronal sections through the medial region of the ME of $EGFP^+$/GnRH1 rats immunoreactive to GnRH subtypes are shown. (*A* and *B*) Cy3-labeled (red) fibers immunoreactive to GnRH1 (LRH 13) (*A*) or GnRH2 (aCII6) (*B*). $EGFP^-$ fibers coexpressing either nonmammalian GnRH appear in yellow. (*C*) Cy3-labeled GnRH2 (aCII6) fibers (red) in close contact with $EGFP^+$/GnRH1 soma (green) in the septal–preoptic area are shown. (Scale bars: *A* and *B*, 100 μm; C, 50 μm.)

Septal–Preoptic Hypothalamus $EGFP^+$/GnRH Neurons. The present results show that the $EGFP^+$/GnRH1 neurons in the septal–preoptic hypothalamus are the bona fide GnRH neurons; they synthesize the authentic GnRH1 and are detected by GnRH1 antisera. Therefore, the expression of EGFP–GnRH1 transgene in the septal–preoptic hypothalamus is restricted to the GnRH1 population described in the rat brain (1). The role of GnRH1 is evolutionarily conserved. GnRH1 functions as a hypophysiotropic hormone for the control of gonadotropin release and is crucial for reproduction throughout the vertebrate species (1, 15).

In the extrahypothalamic area, $EGFP^+$/GnRH1 soma and fibers were seen in the medial HB similar to GnRH2-like immunoreactivity in the musk shrew (31). The medial HB has been implicated in the regulation of female sexual receptivity in

rodents (32) and courtship behavior with associated increase in GnRH-containing mast cells in ringdoves and rats (1, 33).

Septal–Preoptic Hypothalamus EGFP$^-$/GnRH Neurons. In the septal–preoptic hypothalamus, ≈80% of neurons immunoreactive to GnRH1 were EGFP$^+$, but the remaining 20% of GnRH1 neurons were EGFP$^-$. Whether EGFP$^-$ neurons represent a second population of septal–preoptic hypothalamic GnRH neurons, which synthesize a distinct GnRH gene product as in advance teleost and in the guinea pig (15, 34), or contain a posttranscriptionally modified hydroxyprolinated GnRH molecule (35) or GnRH fragments rather than fully mature GnRH1 (8) whose spatiotemporal origin might be different from the placodal origin of GnRH1 neurons (8–10, 15) remains to be determined because a genomewide search failed to detect homologies to GnRH2, GnRH3, and lamprey III GnRH peptide or their ORFs in the rat and mouse databases (36). Therefore, GnRH2, GnRH3, and lamprey III GnRH immunoreactivity in the brain of rodents (16, 17, 37) is questionable, and the role of lamprey III GnRH in the control of follicle-stimulating hormone is debatable (37, 38).

We speculate that the EGFP–GnRH transgene is incapable of exhaustive targeting of the total GnRH1 neuronal population or EGFP$^-$ neurons might express lower levels of the fusion protein, which do not produce visible levels of fluorescence and, therefore, remain undetectable. Alternatively, it is also possible that the synthesis of GnRH in EGFP$^-$ neurons in the forebrain is directed by different segments of the GnRH promoter. The existence of two independent promoter regions directing tissue-specific expression of human GnRH gene has been characterized (39). These two GnRH promoters have differential usage: two nonoverlapping 5′ control elements, each containing only one of the two transcriptional start sites are capable of directing reporter gene expression in tumor cells derived from reproductive tissues or hypothalamic neurons (39). Similarly, in rats, two regulatory regions in the GnRH 5′ flanking DNA have been identified as essential for cell type-specific expression in hypothalamic neurons: a 300-bp enhancer and a 173-bp proximal promoter (40). It is, therefore, conceivable that different promoter segments can direct GnRH synthesis in EGFP$^+$ and EGFP$^-$ neuronal subpopulations in the rat.

Midbrain Central Gray. Up to now, the most accepted view recognizes GnRH2 as phylogenetically the conserved GnRH isoform, synthesized by neurons localized exclusively in the midbrain (13–15, 18). Biochemical assays have shown the presence of GnRH2 in the brain of all vertebrate species studied to date, but neurons expressing GnRH2 mRNA and peptide have been successfully localized in the midbrain of only teleost and primitive placental mammals (15, 41). The presence of GnRH2 neurons in the midbrain of higher vertebrates including rodents remains an enigma. So far, two reports (42, 43) have shown GnRH2 neurons in the midbrain of rodents, which appear to be false positive based on the following reasons. First, although using the same GnRH2 antiserum (aCII6), the two reports show different cell populations in the rodent midbrain as GnRH2-immunopositive. According to the reports, the cells are either scattered along the Aq in the midbrain (42) or reside in the oculomotor and red nuclei (43). Second, the GnRH2 neurons shown in the midbrain (42) morphologically do not appear as typical neurons. Third, the GnRH2 antiserum (aCII6) used in the two studies has been conjugated to BSA, which those authors did not attempt to immunoneutralize (42, 43), causing possible false-positive immunoreaction. Using three different GnRH2 antisera (ISP-II, 1458, and aCII6), we did not find GnRH2-immunopositive soma in the midbrain in our study. Nonspecific GnRH2 immunoreactivity was detected in the oculomotor and red nuclei of rats and in the oculomotor nucleus of teleosts (unpublished observation). Some might argue that the lack of immunopositive GnRH2 cells in the midbrain is caused by technical limitation to detect low levels of GnRH2 peptide or rapid turnover of the peptide. However, the immunocytochemical approach used in this study is well established in our laboratory at Nippon Medical School and has been used to demonstrate GnRH2-immunopositive soma and fibers in teleosts along with successful immunoneutralization (26). In addition, increasing the antiserum concentration or colchicine should have blocked axonal transport of GnRH2; if there were any GnRH2-synthesizing neurons in the midbrain, they would be visible. However, they were not. Thus, in rodents, GnRH2 peptide is probably not transcribed in the midbrain.

Administration of GnRH1 into the midbrain can enhance sexual behavior in female rats (20). Cells in the midbrain could be targets of GnRH1, which is supported by the presence of GnRH1-immunopositive and EGFP$^+$ fiber terminals beneath the ependymal walls of the Aq in the midbrain. Because high doses of GnRH1 were needed to induce lordosis (20), GnRH1 receptors in the midbrain may be low in abundance or exogenous GnRH1 might have acted via the type II GnRH receptors, which have been hypothesized to be involved in behavioral regulation (18). Indeed, GnRH2 is more potent than GnRH1 in stimulating reproductive behaviors in many vertebrates (15, 18, 44–46).

GnRH Fibers. The most conspicuous EGFP$^-$/GnRH1 and GnRH subtype-immunopositive fibers were seen in the OVLT and the caudal ME, suggesting the classical role of GnRH as a hypophysiotropic hormone for the regulation of gonadotropin release. The distribution of EGFP$^+$/GnRH1 and GnRH subtype-immunopositive fibers throughout the septal–preoptic hypothalamus, beneath the ependymal walls of the third ventricle, and surrounding the Aq of the midbrain is consistent with the proposed role of GnRH as a neuromodulator (18). Axosomatic and axodendritic synapses between GnRH1 elements have been reported in the rat and rhesus monkey (1, 47). We now show GnRH fiber contacts between EGFP$^+$ and EGFP$^-$ neurons, which may assist in the coordination of neuroendocrine and neuromodulatory actions of GnRH1.

We thank Dr. M. Kato for providing the transgenic rats. Generous gifts of antibodies from many colleagues (listed in *Materials and Methods*) are also acknowledged. This work was supported in part by Ministry of Education, Culture, Sports, Science, and Technology Grants 14580777 (to I.S.P.), 14370025 and 16086210 (to Y.S.), and Ministry of Health, Labour and Welfare Grant H16-Kagaku-002 (to I.S.P.). The Leica Image Analysis System was purchased with a grant from Japanese Ministry of Education and Science for independent colleges and universities (2000).

1. Silverman, A. J., Livne, I. & Witkin, J. W. (1994) in *The Physiology of Reproduction*, eds. Knobil, E. & Neill, J. D. (Raven, New York), 2nd Ed., pp. 1683–1709.
2. Jennes, L. & Stumpf, W. E. (1986) *Neuroscience* **18,** 403–416.
3. Silverman, A. J., Jhamandas, J. H. & Renaud, L. P. (1987) *J. Neurosci.* **7,** 2312–2319.
4. Merchenthaler, I., Setalo, G., Csontos, C., Petrusz, P., Flerko, B. & Negro-Vilar, A. (1989) *Endocrinology* **125,** 2812–2821.
5. Witkin, J. W. (1990) *Neuroscience* **37,** 501–506.
6. Rajendren, G. (2001) *Brain Res.* **918,** 74–79.
7. Hiatt, E. S., Brunetta, P. G., Seiler, G. R., Barney, S. A., Selles, W. D., Wooledge, K. H. & King, J. C. (1992) *Endocrinology* **130,** 1030–1043.
8. Terasawa, E., Busser, B. W., Luchansky, L. L., Sherwood, N. M., Jennes, L., Millar, R. P., Glucksman, M. J. & Roberts, J. L. (2001) *J. Comp. Neurol.* **439,** 491–504.
9. Skynner, M. J., Slater, R., Sim, J. A., Allen, N. D. & Herbison, A. E. (1999) *J. Neurosci.* **19,** 5955–5966.

10. Schwanzel-Fukuda, M. & Pfaff, D. W. (1989) *Nature* **338,** 161–164.
11. Herbison, A. E. & Pape, J. R. (2001) *Front. Neuroendocrinol.* **22,** 292–308.
12. Gore, A. C. (2002) *GnRH: The Master Molecule of Reproduction* (Kluwer, Dordrecht, The Netherlands).
13. Sherwood, N. M., Schalburg, K. V. & Lescheid, D. W. (1997) in *GnRH Neurons: Gene to Behavior*, eds. Parhar, I. S. & Sakuma, Y. (Brain Shuppan, Tokyo), pp. 3–25.
14. King, J. A. & Millar, R. P. (1997) in *GnRH Neurons: Gene to Behavior*, eds. Parhar, I. S. & Sakuma, Y. (Brain Shuppan, Tokyo), pp. 51–77.
15. Parhar, I. S. (2002) *Prog. Brain Res.* **141,** 3–17.
16. Yahalom, D., Chen, A., Ben-Aroya, N., Rahimipour, S., Kaganovsky, E., Okon, E., Fridkin, M. & Koch, Y. (1999) *FEBS Lett.* **463,** 289–294.
17. Montaner, A. D., Affanni, J. M., King, J. A., Bianchini, J. J., Tonarelli, G. & Somoza, G. M. (1999) *Cell. Mol. Neurobiol.* **19,** 635–651.
18. Millar, R. P. (2003) *Trends Endocrinol. Metab.* **14,** 35–43.
19. Pfaff, D. W. (1973) *Science* **182,** 1148–1149.
20. Sakuma, Y. & Pfaff, D. W. (1980) *Nature* **283,** 566–567.
21. Kato, M., Ui-Tei, K., Watanabe, M. & Sakuma, Y. (2003) *Endocrinology* **144,** 5118–5125.
22. Park, M. K. & Wakabayashi, K. (1986) *Endocrinol. Jpn.* **33,** 257–272.
23. Bläher, S., King, J. A. & Kuenzel, W. J. (1989) *Histochemistry* **93,** 39–48.
24. Senthilkumaran, B., Okuzawa, K., Gen, K., Ookura, T. & Kagawa, H. (1999) *J. Neuroendocrinol.* **11,** 181–186.
25. Paxinos, G. & Watson, C. (1997) *The Rat Brain in Stereotaxic Coordinates* (Academic, San Diego), 3rd Ed.
26. Parhar, I. S., Pfaff, D. W. & Schwanzel-Fukuda, M. (1996) *Brain Res. Mol. Brain Res.* **41,** 216–227.
27. Wu, T. J., Gibson, M. J. & Silverman, A. J. (1995) *J. Neuroendocrinol.* **7,** 899–902.
28. Richardson, H. N., Parfitt, D. B., Thompson, R. C. & Sisk, C. L. (2002) *J. Neuroendocrinol.* **14,** 375–383.
29. Dellovade, T. L., Hunter, E. & Rissman, E. F. (1995) *Neuroendocrinology* **62,** 385–395.
30. Spergel, D. J., Kruth, U., Shimshek, D. R., Sprengel, R. & Seeburg, P. H. (2001) *Prog. Neurobiol.* **63,** 673–686.
31. Rissman, E. F. (1996) *Biol. Reprod.* **54,** 413–419.
32. Swanson, L. W. & Sawchenko, P. E. (1983) *Annu. Rev. Neurosci.* **6,** 269–324.
33. Khalil, M. H., Silverman, A. J. & Silver, R. (2003) *J. Neurobiol.* **56,** 113–124.
34. Jimenez-Linan, M., Rubin, B. S. & King, J. C. (1997) *Endocrinology* **138,** 4123–4130.
35. Gautron, J. P., Pattou, E., Bauer, K. & Kordon, C. (1991) *Neurochem. Int.* **18,** 221–235.
36. Morgan, K. & Millar, R. P. (2004) *Gen. Comp. Endocrinol.* **139,** 191–197.
37. McCann, S. M., Karanth, S., Mastronardi, C. A., Dees, W. L., Childs, G., Miller, B., Sower, S. & Yu, W. H. (2002) *Prog. Brain Res.* **141,** 151–164.
38. Kovacs, M., Seprodi, J., Koppan, M., Horvath, J. E., Vincze, B., Teplan, I. & Flerko, B. (2002) *J. Neuroendocrinol.* **14,** 647–655.
39. Dong, K.-W., Yu, K.-L., Chen, Z.-G., Chen, Y.-D. & Roberts, J. L. (1997) *Endocrinology* **138,** 2754–2762.
40. Lawson, M. A., Macconell, L. A., Kim, J., Powl, B. T., Nelson, S. B. & Mellon, P. L. (2002) *Endocrinology* **143,** 1404–1412.
41. Rissman, E. F., Alones, V. E., Craig-Veit, C. B. & Millam, J. R. (1995) *J. Comp. Neurol.* **357,** 524–531.
42. Gestrin, E. D., White, R. B. & Fernald, R. D. (1999) *FEBS Lett.* **448,** 289–291.
43. Chen, A., Yahalom, D., Ben-Aroya, N., Kaganovsky, E., Okon, E. & Koch, Y. (1998) *FEBS Lett.* **435,** 199–203.
44. Volkoff, H. & Peter, R. E. (1999) *Gen. Comp. Endocrinol.* **116,** 347–355.
45. Maney, D. L., Richardson, R. D. & Wingfield, J. C. (1997) *Horm. Behav.* **32,** 11–18.
46. Kauffman, A. S. & Rissman, E. F. (2004) *Endocrinology* **145,** 3639–3646.
47. Witkin, J. W. (1999) *Microsc. Res. Tech.* **44,** 11–18.

Available online at www.sciencedirect.com
SCIENCE DIRECT®
Biochemical and Biophysical Research Communications 336 (2005) 536–543
BBRC
www.elsevier.com/locate/ybbrc

Cloning and functional analysis of promoters of three GnRH genes in a cichlid

Takashi Kitahashi, Hideki Sato [1], Yasuo Sakuma, Ishwar S. Parhar *

Department of Physiology, Nippon Medical School, Sendagi, Tokyo 113-8602, Japan

Received 27 July 2005
Available online 25 August 2005

Abstract

Mechanisms regulating gonadotropin-releasing hormone (GnRH) types, a key molecule for reproductive physiology, remain unclear. In the present study, we cloned the promoters of GnRH1, GnRH2, and GnRH3 genes in the tilapia, *Oreochromis niloticus*; and found putative binding sites for glucocorticoid receptors, Sp1, C/EBP, GATA, and Oct-1, but not for androgen receptors in all three GnRH promoters using computer analysis. The presence of binding sites for progesterone receptors in GnRH1, estrogen receptors in GnRH1 and GnRH2, and thyroid hormone receptors in GnRH1 and GnRH3 suggests direct action of steroid hormones on GnRH types. Our observation of SOX and LINE-like sequences exclusively in GnRH1, COUP in GnRH2, and retinoid X receptors in GnRH3 suggests their role in sexual differentiation, midbrain segmentation, and visual cue integration, respectively. Thus, the characteristic binding sites for nuclear receptors and transcription factors support the notion that each GnRH type is regulated differently and has distinct physiological roles.
© 2005 Elsevier Inc. All rights reserved.

Keywords: Transcription factors; Steroid hormones; Receptors; Tilapia; *Oreochromis niloticus*; Reproduction; Sex

Gonadotropin-releasing hormone (GnRH) was originally isolated from the porcine hypothalamus [1] as a physiological-releasing hormone of luteinizing hormone and follicle-stimulating hormone in the pituitary gland. Thereafter, the presence of GnRH has been confirmed in a wide range of vertebrate species, and more than 17 forms of GnRHs have been identified to date [2]. It is well documented that most vertebrate species possess two (hypothalamus, GnRH1; midbrain, GnRH2) or, as in some teleosts, three GnRH types (olfactory bulbs, GnRH3) in a single brain [3]. The expression of GnRH genes in a variety of peripheral tissues [4] and the existence of multiple GnRH receptor types [5,6] in a single species suggest that each GnRH type has more than one physiological role and that more than one physiological signal regulates the functioning of GnRH neurons. Indeed, a number of neurotransmitters and steroid hormones have been reported to control GnRH1 neurons [7,8]. However, the exact regulatory mechanism(s) controlling the expression of GnRH1, GnRH2, and GnRH3 genes still remains unclear [9–12]. Understanding the regulatory mechanisms of GnRH genes will expand our knowledge of GnRH neuron physiology and reproduction. Therefore, we cloned the promoters of GnRH1, GnRH2, and GnRH3 genes in the tilapia, *Oreochromis niloticus*, a cichlid species in which three GnRH types have been identified in the brain [12]. Further, we analyzed potential regulatory motifs in the three promoters, which could provide useful information to understand GnRH1, GnRH2, and GnRH3 gene regulation and function.

Materials and methods

Tilapia genomic library. A tilapia genomic library, constructed in Lambda Fix-II vector (Stratagene, La Jolla, CA, USA), was a kind gift from Dr. T. Kobayashi (National Institute for Basic Biology, Okazaki,

* Corresponding author. Fax: +81 3 5685 3055.
E-mail address: ishwar@nms.ac.jp (I.S. Parhar).
[1] Present address: Institute for Frontier Medical Sciences, Kyoto University, Sakyo-ku, Kyoto 606-8507, Japan.

0006-291X/$ - see front matter © 2005 Elsevier Inc. All rights reserved.
doi:10.1016/j.bbrc.2005.08.122

Japan), which was amplified in XL-1 Blue MRA P2 selective host cells (Stratagene) and used in the present experiments.

Probe construction. To screen the tilapia genomic library, primers for GnRH types were designed from known nucleotide sequences of tilapia GnRH cDNAs (GenBank Accession Nos.: GnRH1, AB101665; GnRH2, AB101666; and GnRH3, AB101667). The primer sequences for GnRH1 (G1Fa and G1R), GnRH2 (G2Fa and G2R), and GnRH3 (G3Fa and G3R) are given in Table 1. The polymerase chain reaction (PCR) mixture consisted of 942 ng of tilapia muscle genomic DNA, 1× TaqMan buffer A, 0.25 mM dNTPs, 1 μM each forward and reverse primer set, and 1.25 U (0.25 μl) of AmpliTaq Gold DNA polymerase (Applied Biosystems, CA, USA) in 50 μl of final volume. The PCR was carried out at 94 °C for 10 min, 30 cycles of 94 °C for 30 s, 55 °C for 30 s, and 72 °C for 1 min, and finally 72 °C for 7 min in a GeneAmp PCR System 9700 (Applied Biosystems). After purification with SUPREC-02 (TAKARA BIO, Shiga, Japan), 1/20 volume of the PCR products were used for nested PCR using GnRH1 (G1Fb and G1R), GnRH2 (G2Fb and G2R), and GnRH3 (G3Fb and G3R) primer sets (Table 1) with the same conditions as above. The PCR fragments were cloned into a pGEM-T Easy vector (Promega, WI, USA). Nucleotide sequences of the clones were determined with an ABI PRISM 310 Genetic Analyzer, BigDye Terminator v3.1 Cycle Sequencing Kit and Sequence Analysis Software (Applied Biosystems). To prepare GnRH hybridization probes, PCR was performed with the clones and specific primer sets (GnRH1: G1Fb and G1R; GnRH2: G2Fb and G2R; GnRH3: G3Fb and G3R) and the PCR products were purified using SUPREC-02 (TAKARA BIO).

Isolation of GnRH genomic clones. To identify which of the library fractions contained GnRH1, GnRH2, and GnRH3 genes, the genomic library was screened by PCR using specific primer sets: GnRH1 (G1Fa and G1R), GnRH2 (G2Fa and G2R), and GnRH3 (G3Fb and G3R) (Table 1). An aliquot of each of the 25 library fractions was amplified in a reaction mixture containing 1× polymerase reaction buffer, 0.2 mM dNTPs, 0.5 μM each forward and reverse primer set, and 1.25 U (0.25 μl) Tth DNA polymerase (Promega) in a 50 μl final volume. The PCR was carried out at 94 °C for 5 min, 40 cycles of 94 °C for 30 s, 55 °C for 30 s, and 72 °C for 1 min, and finally at 72 °C for 7 min. PCR products were electrophoresed on 0.8% agarose gel, detected by staining with ethidium bromide, and visualized by illumination with UV light.

Each library fraction that was identified to contain GnRH1, GnRH2 or GnRH3 gene was screened by plaque hybridization technique [13]. To use as a hybridization probe, the PCR products of each GnRH gene described above were labeled using ECL Direct Nucleic Acid Labeling and Detection System (Amersham Biosciences, Piscataway, NJ, USA) according to the manufacturer's protocol. Pre-hybridization and hybridization were carried out at 42 °C for 1 h and 42 °C for 16 h, respectively. Hybridization membranes were washed twice at 42 °C for 30 min in washing buffer containing 6 M urea, 0.4% sodium dodecyl sulfate, and 0.5× SSC (7.5 mM sodium citrate and 75 mM sodium chloride) and then rinsed in 2× SSC (30 mM sodium citrate and 300 mM sodium chloride) at room temperature for 5 min. Detection was carried out at room temperature for 1 min using ECL detection reagents. Positive phage clones containing GnRH1, GnRH2, and GnRH3 genes were isolated and DNAs of the phage clones were extracted using QIAGEN Lambda Mini Kit (QIAGEN, Hilden, Germany). Nucleotide sequences of GnRH genes in the clones were verified using sequencing primers that were used for probe construction. Additional sequencing primers were designed from the obtained sequences and further sequencing steps were performed by primer walking in both directions.

Table 1
Nucleotide sequences of forward (F) and reverse (R) primers

Primer	Sequence
G1Fa	agaagctttatcctcagaat
G1Fb	gggatctggacaacttctca
G1R	ttcttgaatgtccggtgtc
G2Fa	gactaaggtgggaatatcat
G2Fb	gagctggactcctttgggac
G2R	acaaaatcacgtcaaggcag
G3Fa	ttctaatggaagcaggcagc
G3Fb	aagagaagtgtgggagagct
G3R	gtgctgctaataatgatgta

Computer analysis. Exons were predicted by comparing the corresponding cDNA sequence with each GnRH gene. The sequence data were analyzed by a genetic information-processing program, GENETYX (Software Development, Tokyo, Japan). Potential transcription factor binding sites, primarily nuclear receptor response elements, were identified by AliBaba 2.1 program (http://www.gene-regulation.com/) along the 4.0–4.5 kbp upstream of the transcription start site. BLAST program (http://www.ncbi.nlm.nih.gov/BLAST/) was used for sequence comparison between tilapia GnRH promoters and database sequences of other teleost genomes.

Results

Structure of three GnRH genes

The cloned promoter for GnRH1, GnRH2, and GnRH3 genes was about 4, 4.5, and 4.5 kbp, the GnRH gene was 0.8, 1.5, and 1.1 kbp, and the 3′ flanking region was 0.2, 0.3, and 0.3 kbp, respectively. The total nucleotide sequences determined for GnRH1, GnRH2, and GnRH3 genes were 5124, 6296, and 5953 bp, respectively. These sequences have been deposited in the GenBank (Accession Nos.: GnRH1, AB104861; GnRH2, AB104862; GnRH3, AB104863).

Gene structure

All three GnRH genes have 4 exons and 3 introns. In each gene, exon 1 encodes the 5′-untranslated region (UTR) and exon 2 encodes the signal peptide, the GnRH decapeptide, a Gly-Lys-Arg amidation cleavage site, and the N-terminus of GnRH-associated peptide (GAP). Exon 3 encodes the middle portion of the GAP and exon 4 contains the C-terminus of GAP and the 3′-UTR (Fig. 1). A typical splice site, which is characterized as GT (donor) and AG (acceptor), exists in every intron of the three GnRH genes. Nucleotide sequences encoding GnRH decapeptides showed 63.3% similarity between GnRH1 and GnRH2, 70.0% between GnRH1 and GnRH3, and 76.7% between GnRH2 and GnRH3. When compared between species, nucleotide sequences encoding tilapia GnRH decapeptides showed

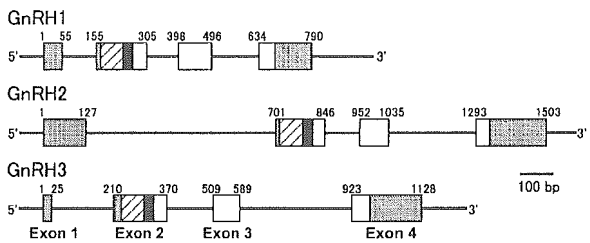

Fig. 1. Schematic diagram showing the genomic structure of GnRH1, GnRH2, and GnRH3 genes of tilapia. The coding sequence for the signal peptide is hatched; the GnRH decapeptide is in black; the processing site and the GAP are in white; and the 5′ and 3′ untranslated regions are shown in stippled box. Introns are shown as lines. The numbers on the shoulders indicate nucleotide positions of exon boundaries.

80.0%, 93.3%, and 100% homology with those encoding GnRH1, GnRH2, and GnRH3 in the medaka, *Oryzias latipes*, respectively. Only 1 nucleotide difference was found in GnRH1 coding region when compared with an evolutionally close species, the *Haplochromis burtoni*. Nucleotide sequences encoding GAP were less conserved, showing 49.5% similarity between GnRH1 and GnRH2, 47.2% between GnRH1 and GnRH3, and 49.1% between GnRH2 and GnRH3. When compared between species, nucleotide sequences encoding tilapia GAPs showed 66.5%, 81.1%, and 86.8% homology with those encoding medaka GnRH1-GAP, GnRH2-GAP, and GnRH3-GAP, respectively. Comparison with *H. burtoni* GnRH1-GAP, GnRH2-GAP, and GnRH3-GAP showed 97.9–99.4% homology.

GnRH1 promoter sequence

The promoter region from transcription start site to −90 bp showed comparatively high homology (67.8%) between tilapia and medaka (Fig. 2). However, the promoter region from −90 to −4097 bp of GnRH1 gene in tilapia showed low homology with the corresponding region in the medaka (Fig. 2). When compared with a closely related species, the *H. burtoni*, the promoter region from −736 bp of tilapia GnRH1 gene had no homology (Fig. 2). The promoter region from −737 to −1927 bp had high homology (95.5%) with chicken repeat 1 (CR1)-like long interspersed repetitive elements (LINE) of tilapia (AY495714S2) (Fig. 3 region a), and with putative LINE-like retrotransposon of torafugu, *Takifugu rubripes* (TRU459419) from −1614 to −4097 bp (Fig. 3 region b). The nucleotide sequence from −2833 to −3732 bp had high homology (93.2%) to two regions lying between C-type lectin natural killer cell-like protein (KLR) 1 gene and KLR2 pseudogene of tilapia (AY495714S1) (Fig. 3 region c).

Binding sites for several different nuclear receptors (estrogen receptor, ER; progesterone receptor, PR; glucocorticoid receptor, GR; and thyroid hormone receptor, TR) were found in the promoter region between positions −70 and −4050 bp (Fig. 2). Several putative binding sites for Sp1 and CCAAT/enhancer binding protein (C/EBP) were found in the promoter region of GnRH1 gene, which also included binding sites for transcription factors, myogenic factor-3 (Myf-3), myoblast determination protein (MyoD), two octamer-binding transcription factor-1 (Oct-1), and SRY-box-2 (SOX-2) at positions of −430, −1005, −3152, −3555, and −3413 bp from the transcription initiation site, respectively (Fig. 2). The number of putative binding sites for nuclear receptors and transcription factors is given in Table 2.

GnRH2 promoter sequence

Within the promoter region of tilapia GnRH2 gene, nucleotide sequence from −1530 to −1900 bp showed high homology (79.2%) with the corresponding region of GnRH2 gene of medaka (Fig. 4).

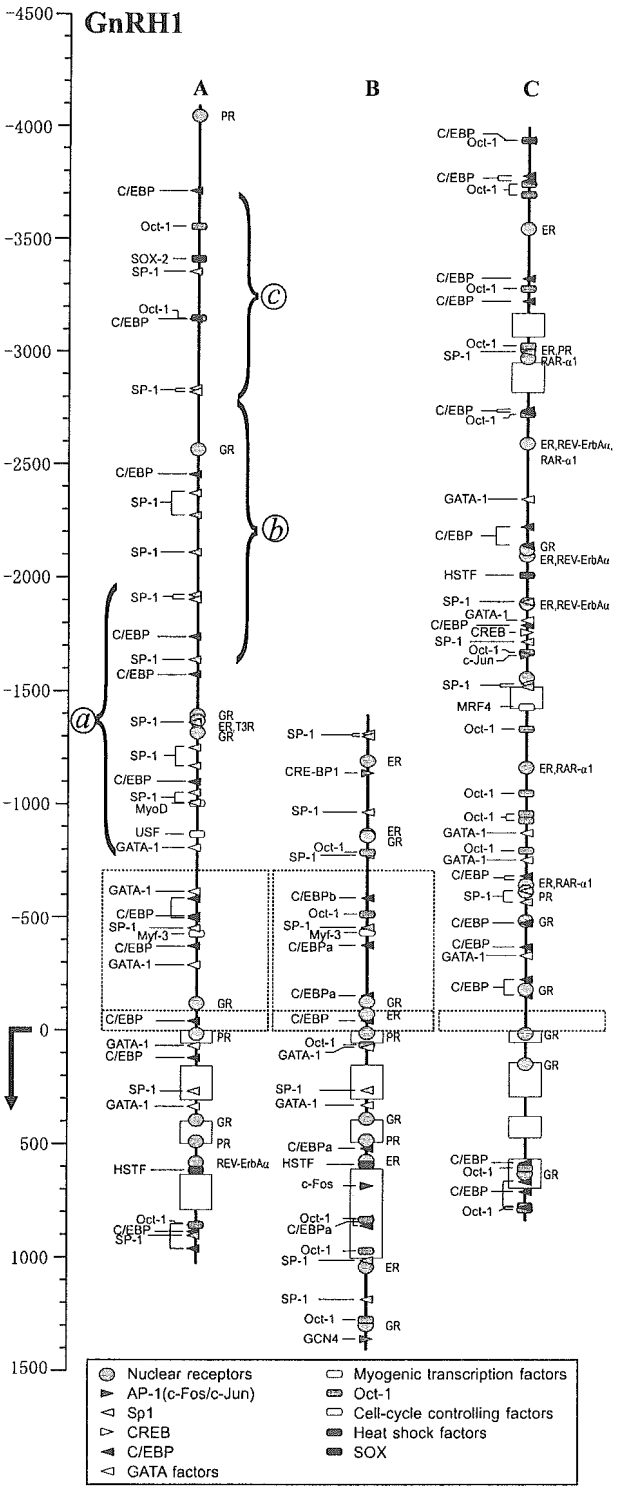

Fig. 2. Schematic representation of putative regulatory motifs in the GnRH1 gene of tilapia (A), *H. burtoni* (B), and medaka (C). Green boxes indicate exons, and boxes with broken lines indicate regions that are conserved among species. Regions indicated by a, b, and c correspond to those in Fig. 3. The *H. burtoni* and the medaka GnRH1 gene sequences were obtained from the GenBank (Accession Nos.: AF076961 and AB074499, respectively). The scale, as distance from the transcription start site (position = 1; bend arrow), is given on the left.

Table 2
Predicted binding sites in the promoter regions of tilapia GnRH genes

Gene	ER	AR	PR	GR	TR	RAR/RXR	COUP	AP-1	Sp1	CREB	C/EBP	GATA	Myo	Oct-1	Cell- cycle	HSF	SOX
GnRH1	1	0	1	4	1	0	0	0	15	0	11	3	2	2	1	0	1
GnRH2	4	0	0	4	0	1	1	1	10	0	14	1	0	5	1	0	0
GnRH3	0	0	0	6	2	3	0	2	6	0	9	5	2	9	0	0	0

Putative binding sites as identified by AliBaba 2.1. ER, estrogen receptors; AR, androgen receptors; PR, progesterone receptors; GR, glucocorticoid receptors; TR, thyroid hormone receptors; RAR, retinoic acid receptors; RXR, retinoid X receptors; COUP, chick ovalbumin upstream promoter-transcription factor; CREB, cAMP response element binding protein; C/EBP, CCAAT/enhancer binding proteins; GATA, GATA binding proteins; Myo, myogenic transcription factors; Oct-1, octamer-binding transcription factor-1; Cell-cycle, cell-cycle controlling factors; HSF, heat shock factors; SOX, SRY-boxes.

A cluster of ER and GR binding sites was found in the distal part of the promoter between positions −2662 and −4156 bp (Fig. 4). Binding sites for Sp1, C/EBP, Oct-1, AP-1, retinoic acid receptor (RAR), ER, and chick ovalbumin upstream promoter-transcription factor (COUP) were found in the proximal part (−100 to −1200 bp) of GnRH2 promoter. Binding sites for myogenic transcription factors, heat shock factors (HSF), and SOX were absent in GnRH2 promoter (Table 2).

GnRH3 promoter sequence

Several regions in the promoter of tilapia GnRH3 gene showed high homology (67.6–90.0%) to the corresponding regions of medaka GnRH3 gene (Fig. 5). The promoter region from positions −2096 to −4560 bp contained an open-reading frame of a gene, which encodes protein tyrosine phosphatase ε (Fig. 5).

The promoter of GnRH3 gene contained binding sites for retinoid X receptor (RXR), GR, TR, and RAR but not for ER, AR, or PR (Table 2). Also, binding sites for c-Jun, myogenic transcription factors (myogenin and MRF4), clusters of C/EBP, Sp1, GATA binding protein-1 (GATA-1), and Oct-1 were found in the promoter of GnRH3 gene (Fig. 5).

Discussion

As all known GnRH genes [14], the three GnRH genes of tilapia are composed of four exons and three introns. In each GnRH gene, the GnRH decapeptide is coded by exon 2 and the GAP by exons 2, 3, and 4. High homology of nucleotide sequences encoding GnRH1, GnRH2, and GnRH3 and their respective GAP (>96.7%) was seen between tilapia and another closely related cichlid [14]. When compared with medaka, homology of nucleotide sequences was high in GnRH3 gene and low in GnRH1 gene, suggesting different selective pressure among GnRH genes. The promoter region of each GnRH gene has its own characteristic putative nuclear receptor and transcription factor binding sites, suggesting that each GnRH gene is functionally different and under different regulatory mechanism.

The present study demonstrates for the first time the presence of GR binding sites not only in GnRH1 promoter but also in GnRH2 and GnRH3 promoters. Since glucocorticoids down regulate GnRH1 gene expression ([15], Soga et al., unpublished data) through GR in GnRH1 neurons [16], it is possible that in socially stressed male cichlids the high levels of plasma cortisol ([17], Soga et al., unpublished data) could suppress GnRH1, GnRH2, and GnRH3 gene expression [11] through GR binding sites; and thereby suppress gonadal maturation and reproductive behavior in subordinates of cichlids [18,19].

Testosterone down-regulates GnRH1 and up-regulates GnRH3 in tilapia [9] but has contradictory effects on GnRH1 in several other vertebrate species [20–22]. The absence of AR binding sites in GnRH1, GnRH2, and GnRH3 promoters suggests that androgens regulate all three GnRH genes indirectly through androgen-responsive neurons as in rodents [23]. Alternatively, it is possible that aromatizable androgen regulates GnRH1 and GnRH2 neurons through ERs in GnRH neurons ([24], Parhar et al., unpublished data). The presence of ER binding sites (present study) and the lack of effects of 11-ketotestosterone, a non-aromatizable androgen, on GnRH gene expression support the existence of an estrogenic pathway [10] in GnRH1 and GnRH2 neurons.

The presence of putative binding sites for TR in the promoter of GnRH1 and GnRH3 genes supports the suppression of GnRH3 mRNA by thyroid hormone in tilapia [10] and a direct action of thyroid hormones on GnRH1 neuron as in mammals [25]. Colocalization of TR and ER binding sites suggests possible competitive DNA binding or protein/protein interactions of TR and ER [26], which could influence the effect of E2 and thyroid hormones on GnRH1 gene expression.

Transcription factors such as AP-1 [27], Sp1 [28], C/EBP [29], and GATA [30] interact with ER, and regulate GnRH1 gene expression in GT1-7 cell line [31,32]. In addition, Oct-1, which has an important role in cell-specific expression of GnRH1 gene [33], interacts with GR and is considered to mediate glucocorticoid repression of GnRH1 gene [34]. A similar mechanism could also operate in GnRH2 and GnRH3 neurons, but remains to be seen. Thus, steroid hormones may use a combination of transcription factors, which are specific for the cell type, and bind to specific gene promoters to evoke distinct gene responses in GnRH1, GnRH2, and GnRH3 neurons.

Comparisons between the promoters of GnRH1 gene of tilapia and its evolutionally close relative, *H. burtoni* (short

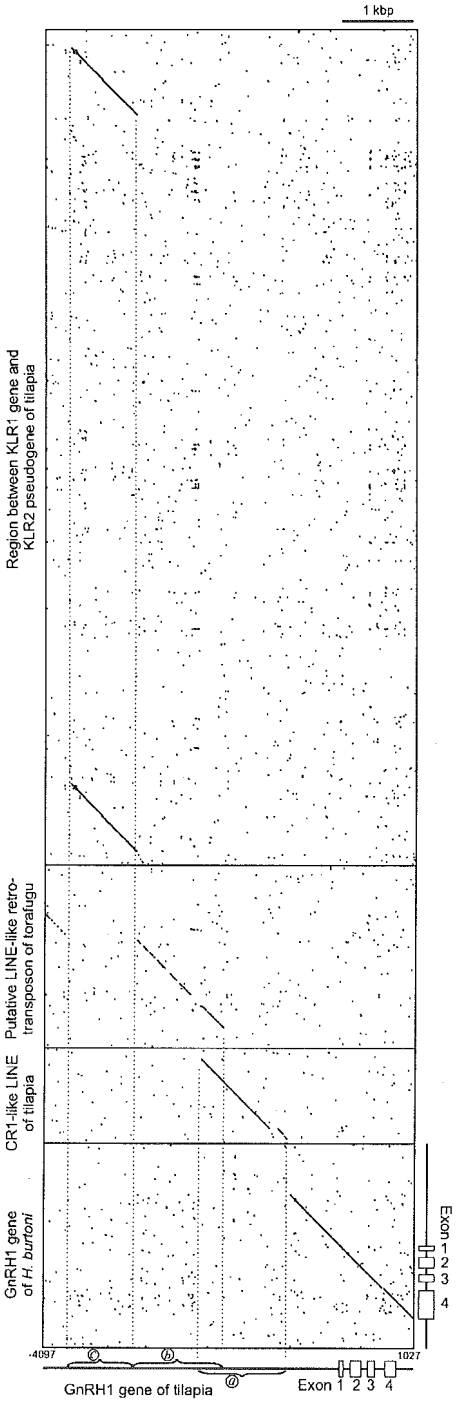

Fig. 3. Harr plot analysis of the GnRH1 gene of tilapia. Sequences represented on the horizontal axis (GnRH1 gene of *H. burtoni*, CR1-like LINE of tilapia, putative LINE-like retrotransposon of torafugu, and the region between KLR1 gene and KLR2 pseudogene of tilapia) were obtained from the GenBank (Accession Nos.: AF076961, AY495714S2, TRU459419, and AY495714S1, respectively). Gene structures of GnRH1 of tilapia and *H. burtoni* are schematically represented on the *X*- and *Y*-axis; exons are boxes while other regions are lines. Each dot represents a position where 14 out of 20 nucleotides of each gene on the *Y*-axis match tilapia GnRH1 gene on the *X*-axis. Regions indicated by a, b, and c correspond to those in Fig. 2. The scale is given in kilo base pairs (kbp).

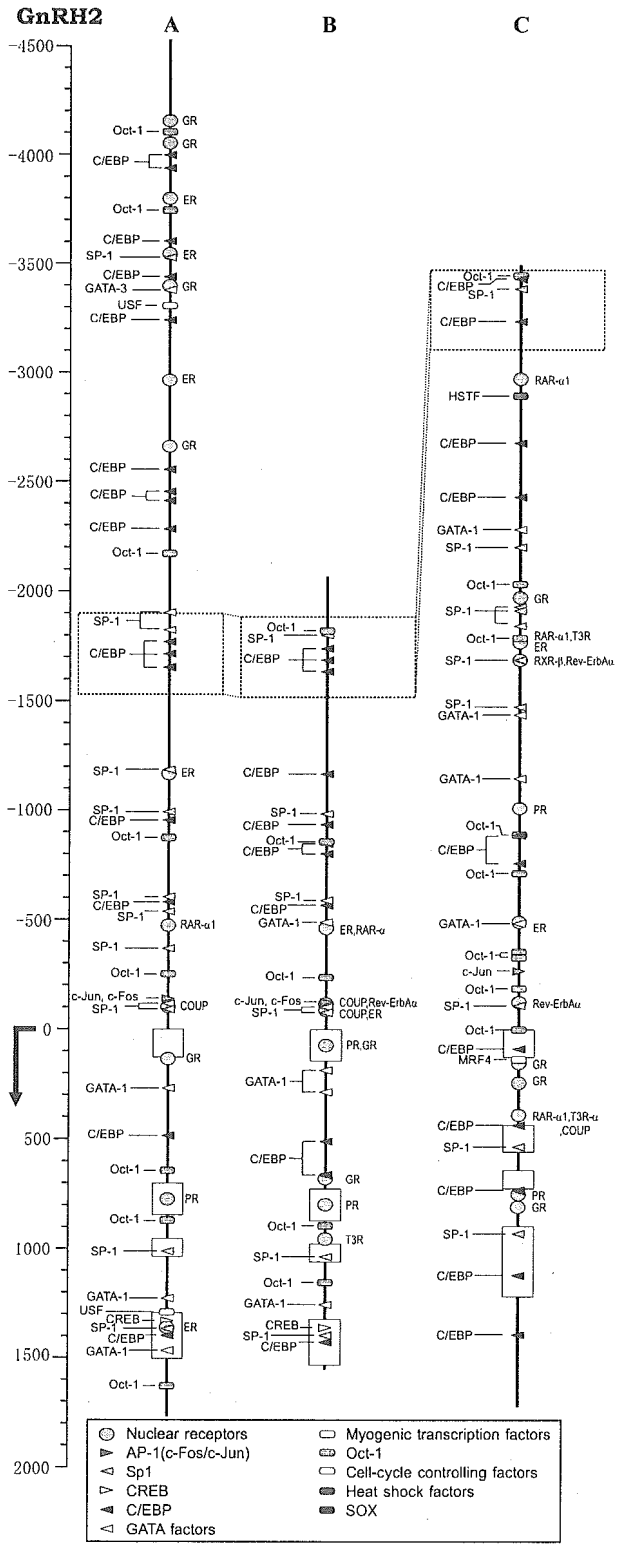

Fig. 4. Schematic representation of putative regulatory motifs in the GnRH2 gene of tilapia (A), *H. burtoni* (B), and medaka (C). Green boxes indicate exons, and boxes with broken lines indicate regions that are conserved among the three species. The *H. burtoni* and the medaka GnRH2 gene sequences were obtained from the GenBank (Accession Nos.: AF076962 and AB074500, respectively). The scale, as distance from the transcription start site (position = 1; bend arrow), is given on the left.

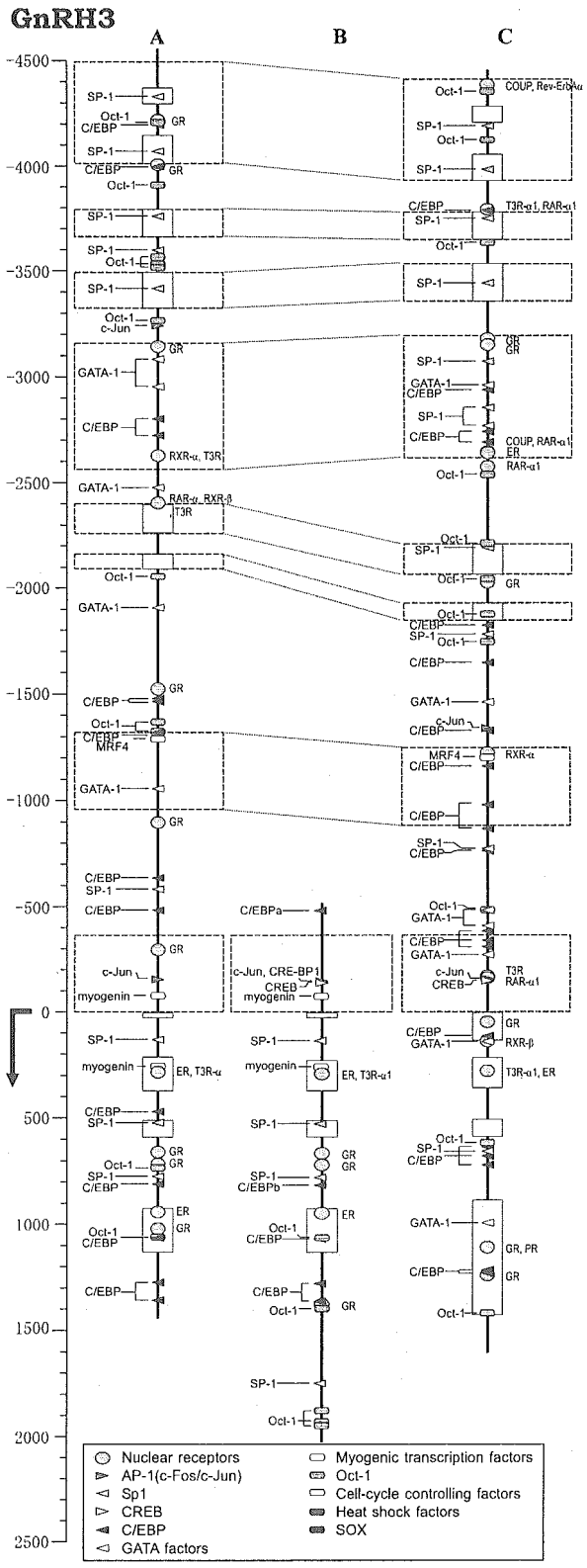

Fig. 5. Schematic representation of putative regulatory motifs in the GnRH3 gene of tilapia (A), *H. burtoni* (B), and medaka (C). Green boxes indicate exons, and boxes with broken lines indicate regions that are conserved among species. The *H. burtoni* and the medaka GnRH3 gene sequences were obtained from the GenBank (Accession Nos.: AF076963 and AB074501, respectively). The scale, as distance from the transcription start site (position = 1; bend arrow), is given on the left.

nucleotide sequence), show insertions or deletions of LINE-like sequences occurred in evolutionally recent past in cichlids. Similar comparisons of GnRH1 promoters between medaka and striped bass (*Morone saxatilis*: AF056314), and between human (*Homo sapiens*: U56735) and mouse (*Mus musculus*: U29674) show several insertions in the striped bass and human or deletions in medaka and mouse GnRH1 promoter (data not shown). These facts suggest that the promoter of GnRH1 gene permitted insertions and deletions of nucleotide sequences during evolution. Thus, the permissiveness of GnRH1 promoter to insert and delete nucleotide sequences, in part, could contribute to the species-specific regulation of GnRH1 gene expression and the diversity in reproductive strategies in vertebrate species.

The presence of binding sites for SOX and PR, and the presence of LINE-like sequences exclusively in GnRH1 promoter are interesting because progesterone is known to regulate SOX [35] and SOX affects promoter activity of LINE-1 [36]. This suggests an integrative role for these motifs/transcription factors in the regulation of GnRH1. Since SOX proteins are involved in sexual and neural differentiation [37], therefore, it is possible that GnRH1 is involved in sexual differentiation [18]. In our earlier study, the absence of influence of progesterone on any of the three GnRH systems in the male tilapia [38] is probably due to the dose, reproductive stage of animals or the lack of estrogen priming, which is essential for GnRH1 synthesis by progesterone [39].

The presence of binding sites for myogenic factors in the promoter of GnRH1 gene provides indirect evidence for the speculative role of GnRH1 and GnRH receptors in skeletal muscle physiology [4,40,41].

The exact physiological function(s) and regulatory mechanism(s) of GnRH2 neurons, located in the midbrain of vertebrates, remain unclear. However, these neurons have been implicated in the control of reproductive behavior [18]. Our observations of a putative COUP binding site specifically in the promoter of GnRH2 gene suggest a novel role for GnRH2. COUP transcription factors have been shown to play an important role in the specification of diencephalic and mesencephalic neuromeres during development [42]. Thus, it will be interesting to observe the role of GnRH2 in midbrain segmentation and/or the role of COUP in the regulation of GnRH2 for reproductive functions.

The presence of putative RAR and RXR binding sites in the promoters of GnRH2 and GnRH3 genes supports the possibility of direct action of retinoic acid and retinoid X on GnRH2 and GnRH3 gene expression as shown for GnRH1 gene in mammals [43]. Further, although GnRH3 neurons have been speculated to innervate the retina in teleost [44], the present study suggests that GnRH2 is also a potential candidate which together with GnRH3 could participate in the integration of visual cues.

The present results show that each GnRH gene in tilapia has a distinct promoter with characteristic putative binding sites for nuclear receptors and transcription factors, which

confirms the idea that each GnRH type is under different regulatory mechanism(s) and has distinct physiological role(s).

Acknowledgments

This work was supported in part by Grants-in-Aid from the Ministry of Education, Culture, Sports, Science and Technology of Japan; Grant No.: 14580777 (to I.S.P.); Grant No.: 4370025 (to Y.S.) and the Ministry of Health, Labour and Welfare; Grant No.: H16-kagaku-002 (to I.S.P.).

References

[1] H. Matsuo, Y. Baba, R.M. Nair, A. Arimura, A.V. Schally, Structure of the porcine LH- and FSH-releasing hormone. I. The proposed amino acid sequence, Biochem. Biophys. Res. Commun. 43 (1971) 1334–1339.

[2] E. Iwakoshi-Ukena, K. Ukena, K. Takuwa-Kuroda, A. Kanda, K. Tsutsui, H. Minakata, Expression and distribution of octopus gonadotropin-releasing hormone in the central nervous system and peripheral organs of the octopus (*Octopus vulgaris*) by in situ hybridization and immunohistochemistry, J. Comp. Neurol. 477 (2004) 310–323.

[3] I.S. Parhar, Cell migration and evolutionary significance of GnRH subtypes, Prog. Brain Res. 141 (2002) 3–17.

[4] K. Okubo, H. Suetake, K. Aida, Expression of two gonadotropin-releasing hormone (GnRH) precursor genes in various tissues of the Japanese eel and evolution of GnRH, Zool. Sci. 16 (1999) 471–478.

[5] R.P. Millar, Z.L. Lu, A.J. Pawson, C.A. Flanagan, K. Morgan, S.R. Maudsley, Gonadotropin-releasing hormone receptors, Endocr. Rev. 25 (2004) 235–275.

[6] I.S. Parhar, S. Ogawa, Y. Sakuma, Three GnRH receptor types in laser-captured single cells of the cichlid pituitary display cellular and functional heterogeneity, Proc. Natl. Acad. Sci. USA (2005).

[7] A.E. Herbison, J.R. Pape, New evidence for estrogen receptors in gonadotropin-releasing hormone neurons, Front. Neuroendocrinol. 22 (2001) 292–308.

[8] A.C. Gore, GnRH: The Master Molecule of Reproduction, Kluwer Academic Publishers, Dordrecht, 2002.

[9] T. Soga, Y. Sakuma, I.S. Parhar, Testosterone differentially regulates expression of GnRH messenger RNAs in the terminal nerve, preoptic and midbrain of male tilapia, Brain Res. Mol. Brain Res. 60 (1998) 13–20.

[10] I.S. Parhar, T. Soga, Y. Sakuma, Thyroid hormone and estrogen regulate brain region-specific messenger ribonucleic acids encoding three gonadotropin-releasing hormone genes in sexually immature male fish, *Oreochromis niloticus*, Endocrinology 141 (2000) 1618–1626.

[11] S. Ogawa, T. Soga, Y. Sakuma, I.S. Parhar, Modulation of GnRH subtypes by social stress and aggressive behavior, Fish Physiol. Biochem. 28 (2003) 49–50.

[12] I.S. Parhar, S. Ogawa, T. Hamada, Y. Sakuma, Single-cell real-time quantitative polymerase chain reaction of immunofluorescently identified neurons of gonadotropin-releasing hormone subtypes in cichlid fish, Endocrinology 144 (2003) 3297–3300.

[13] J. Sambrook, D. Russell, Molecular Cloning, third ed., Cold Spring Harbor Laboratory Press, Cold Spring Harbor, NY, 2001.

[14] R.D. Fernald, R.B. White, Gonadotropin-releasing hormone genes: phylogeny, structure, and functions, Front. Neuroendocrinol. 20 (1999) 224–240.

[15] H.J. Goos, D. Consten, Stress adaptation, cortisol and pubertal development in the male common carp, *Cyprinus carpio*, Mol. Cell. Endocrinol. 197 (2002) 105–116.

[16] C.A. Teitsma, I. Anglade, C. Lethimonier, G. Le Drean, D. Saligaut, B. Ducouret, O. Kah, Glucocorticoid receptor immunoreactivity in neurons and pituitary cells implicated in reproductive functions in rainbow trout: a double immunohistochemical study, Biol. Reprod. 60 (1999) 642–650.

[17] H.E. Fox, S.A. White, M.H. Kao, R.D. Fernald, Stress and dominance in a social fish, J. Neurosci. 17 (1997) 6463–6469.

[18] I.S. Parhar, GnRH in tilapia: three genes, three origins and their roles, in: I.S. Parhar, Y. Sakuma (Eds.), GnRH Neurones: Gene to Behavior, Brain Shuppan, Tokyo, 1997, pp. 99–122.

[19] S.A. White, T. Nguyen, R.D. Fernald, Social regulation of gonadotropin-releasing hormone, J. Exp. Biol. 205 (2002) 2567–2581.

[20] L. Iela, B. D'Aniello, M. Di Meglio, R.K. Rastogi, Influence of gonadectomy and steroid hormone replacement therapy on the gonadotropin-releasing hormone neuronal system in the anterior preoptic area of the frog (*Rana esculenta*) brain, Gen. Comp. Endocrinol. 95 (1994) 422–431.

[21] E.A. Dubois, S. Slob, M.A. Zandbergen, J. Peute, H.J. Goos, Gonadal steroids and the maturation of the species-specific gonadotropin-releasing hormone system in brain and pituitary of the male African catfish (*Clarias gariepinus*), Comp. Biochem. Physiol. B 129 (2001) 381–387.

[22] H.N. Richardson, A.C. Gore, J. Venier, R.D. Romeo, C.L. Sisk, Increased expression of forebrain GnRH mRNA and changes in testosterone negative feedback following pubertal maturation, Mol. Cell. Endocrinol. 214 (2004) 63–70.

[23] I.H. Zwain, A. Arroyo, P. Amato, S.S. Yen, A role for hypothalamic astrocytes in dehydroepiandrosterone and estradiol regulation of gonadotropin-releasing hormone (GnRH) release by GnRH neurons, Neuroendocrinology 75 (2002) 375–383.

[24] S.L. Petersen, E.N. Ottem, C.D. Carpenter, Direct and indirect regulation of gonadotropin-releasing hormone neurons by estradiol, Biol. Reprod. 69 (2003) 1771–1778.

[25] H.T. Jansen, L.S. Lubbers, E. Macchia, L.J. DeGroot, M.N. Lehman, Thyroid hormone receptor (alpha) distribution in hamster and sheep brain: colocalization in gonadotropin-releasing hormone and other identified neurons, Endocrinology 138 (1997) 5039–5047.

[26] T.L. Dellovade, Y.S. Zhu, D.W. Pfaff, Thyroid hormones and estrogen affect oxytocin gene expression in hypothalamic neurons, J. Neuroendocrinol. 11 (1999) 1–10.

[27] K. Paech, P. Webb, G.G. Kuiper, S. Nilsson, J. Gustafsson, P.J. Kushner, T.S. Scanlan, Differential ligand activation of estrogen receptors ERalpha and ERbeta at AP1 sites, Science 277 (1997) 1508–1510.

[28] S. Safe, Transcriptional activation of genes by 17 beta-estradiol through estrogen receptor-Sp1 interactions, Vitam. Horm. 62 (2001) 231–252.

[29] B. Stein, M.X. Yang, Repression of the interleukin-6 promoter by estrogen receptor is mediated by NF-kappa B and C/EBP beta, Mol. Cell. Biol. 15 (1995) 4971–4979.

[30] G.A. Blobel, C.A. Sieff, S.H. Orkin, Ligand-dependent repression of the erythroid transcription factor GATA-1 by the estrogen receptor, Mol. Cell. Biol. 15 (1995) 3147–3153.

[31] M.A. Lawson, D.B. Whyte, P.L. Mellon, GATA factors are essential for activity of the neuron-specific enhancer of the gonadotropin-releasing hormone gene, Mol. Cell. Biol. 16 (1996) 3596–3605.

[32] D.D. Belsham, P.L. Mellon, Transcription factors Oct-1 and C/EBPbeta (CCAAT/enhancer-binding protein-beta) are involved in the glutamate/nitric oxide/cyclic-guanosine 5′-monophosphate-mediated repression of mediated repression of gonadotropin-releasing hormone gene expression, Mol. Endocrinol. 14 (2000) 212–228.

[33] M.E. Clark, P.L. Mellon, The POU homeodomain transcription factor Oct-1 is essential for activity of the gonadotropin-releasing hormone neuron-specific enhancer, Mol. Cell. Biol. 15 (1995) 6169–6177.

[34] U.R. Chandran, D.B. DeFranco, Regulation of gonadotropin-releasing hormone gene transcription, Behav. Brain Res. 105 (1999) 29–36.

[35] J.D. Graham, S.M. Hunt, N. Tran, C.L. Clarke, Regulation of the expression and activity by progestins of a member of the SOX gene family of transcriptional modulators, J. Mol. Endocrinol. 22 (1999) 295–304.
[36] T. Tchenio, J.F. Casella, T. Heidmann, Members of the SRY family regulate the human LINE retrotransposons, Nucleic Acids Res. 28 (2000) 411–415.
[37] M. Wegner, From head to toes: the multiple facets of Sox proteins, Nucleic Acids Res. 27 (1999) 1409–1420.
[38] I.S. Parhar, T. Soga, Y. Sakuma, Quantitative in situ hybridization of three gonadotropin-releasing hormone-encoding mRNAs in castrated and progesterone-treated male tilapia, Gen. Comp. Endocrinol. 112 (1998) 406–414.
[39] K. Kim, B.J. Lee, Y. Park, W.K. Cho, Progesterone increases messenger ribonucleic acid (mRNA) encoding luteinizing hormone releasing hormone (LHRH) level in the hypothalamus of ovariectomized estradiol-primed prepubertal rats, Brain Res. Mol. Brain Res. 6 (1989) 151–158.
[40] S.S. Kakar, L. Jennes, Expression of gonadotropin-releasing hormone and gonadotropin-releasing hormone receptor mRNAs in various non-reproductive human tissues, Cancer Lett. 98 (1995) 57–62.
[41] A. Jodo, H. Ando, A. Urano, Five different types of putative GnRH receptor gene are expressed in the brain of masu salmon (*Oncorhynchus masou*), Zool. Sci. 20 (2003) 1117–1125.
[42] S.Y. Tsai, M.J. Tsai, Chick ovalbumin upstream promoter-transcription factors (COUP-TFs): coming of age, Endocr. Rev. 18 (1997) 229–240.
[43] S. Cho, H. Cho, D. Geum, K. Kim, Retinoic acid regulates gonadotropin-releasing hormone (GnRH) release and gene expression in the rat hypothalamic fragments and GT1-1 neuronal cells in vitro, Brain Res. Mol. Brain Res. 54 (1998) 74–84.
[44] H. Munz, B. Claas, W.E. Stumpf, L. Jennes, Centrifugal innervation of the retina by luteinizing hormone releasing hormone (LHRH)-immunoreactive telencephalic neurons in teleosten fishes, Cell Tissue Res. 222 (1982) 313–323.

ELSEVIER

EXPERIMENTAL HEMATOLOGY

Experimental Hematology ■ (2006) ■

Caloric restriction prevents radiation-induced myeloid leukemia in c3H/HeMs mice and inversely increases incidence of tumor-free death: implications in changes in number of hemopoietic progenitor cells

Kazuko Yoshida[a], Yoko Hirabayashi[b], Fumiko Watanabe[a], Toshihiko Sado[a], and Tohru Inoue[c]

[a]*Radiation Hazards Research Group, National Institute of Radiological Sciences, Chiba, Japan;* [b]*Division of Cellular and Molecular Toxicology and* [c]*Center for Biological Safety and Research, National Institute of Health Sciences, Tokyo, Japan*

[Q2] (Received 9 June 2005; revised 25 October 2005; accepted 30 November 2005)

[Q3] Radiation-induced leukemia was noted as the highest risk factor for mortality among atomic bomb survivors in Hiroshima and Nagasaki [1,2]. Relative risk of leukemia has been estimated to be approximately 6.5, whereas that for other tumors is 1.2 [2]. Experimentally, caloric restriction (CalR) has been found to be only a preventive factor for the risk comparable to epidemiological relevancy in atomic bomb survivors. Thus, timing of restriction seems to be an additional factor that should be taken into account when trying to understand not only the underlying mechanism, but also the epidemiological relevancy of CalR.

Our previous study of CalR using C3H/He mice, which are prone to radiation-induced myeloid leukemia [3], in relation to radiation-induced leukemogenesis showed that CalR led to a significant decrease in the incidence of myeloid leukemias [4]. Furthermore, when timing of CalR between lifetime CalR and postirradiation CalR were compared, onset of myeloid leukemia was significantly delayed in the former compared with the latter, although both resulted in a significant decrease in total incidence of myeloid leukemias. Thus, the present study was designed to elucidate the role of different CalR timings, including preirradiation CalR, in leukemogenic prevention. Possible target cells for radiation leukemogenesis are hemopoietic stem cells, that is, long-term repopulating stem cells [5] and the population of such hemopoietic stem cells changes proportionally in response to different types of progenitor cell [6], such as granulocyte macrophage colony-forming units (CFU-GM) and other progenitors, including splenic colony-forming units (CFU-S) [7,8]. In relation to these, the number of hemopoietic progenitor cells (HPCs), and the kinetics of HPCs, i.e., cell-cycle parameters, were evaluated and compared among the CalR groups as possible markers predict leukemogenesis.

CalR induces a notable decrease in splenic weight and, consequently, in the number of HPCs, which may respond proportionally to the number of hemopoietic stem cells, the potential target cells for myeloid leukemogenesis [9]. In our previous experiments, we observed the effect of CalR throughout the lifespan of mice, which raised the question as to whether risk of leukemogenesis is a function of the number of potential target cells and, consequently, a function of the number of HPCs at the time of irradiation. In the present study, to answer this question, CalR in mice was started at 6 weeks old for the first group until the time of irradiation, at 10 weeks old, and mice were then returned to a regular non-CalR diet. In the other group, restriction was started at 10 weeks old and continued throughout their lifespan. The former treatment was designed to modify the stage of leukemogenesis before irradiation, and the latter to determine the effect of diet on the stage of leukemogenesis after irradiation. We refer to the former treatment as modification of the "initiation stage" of leukemogenesis, because this treatment modifies the number of possible target cells for leukemic initiation; and the latter stage as modification of the "promotion stage" of leukemogenesis, because this treatment modifies proliferation and differentiation of potentially initiated cells after irradiation.

CalR neither more significantly prevented radiation-induced development of neoplasms other than myeloid leukemias nor inversely increased the incidence of any neoplasm. Consequently, because of decreased incidence of myeloid leukemias, incidence of tumor-free death increased.

Materials and methods

Mice

C3H/He mice, which are prone to radiation-induced myeloid leukemia, were used in the present study. Incidence of spontaneous

[Q1] Offprint requests to: Kazuko Yoshida, Radiation Hazards Research Group, National Institute of Radiological Sciences, 4-9-1 Anagawa, Inage-ku, Chiba 263-8555, Japan; E-mail: yosida@nirs.go.jp

0301-472X/06 $–see front matter. Copyright © 2006 International Society for Experimental Hematology. Published by Elsevier Inc.
doi: 10.1016/j.exphem.2005.11.016

myeloid leukemia in C3H/He male mice is 1%, which increased to 23.3% after 3-Gy whole-body x-ray irradiation [3]. Six-week-old male C3H/HeNirsMs mice bred at our institute and released as cohort were used. Mice were housed individually, but were housed in groups if their weights were within 6% to 8% of each other, in environmentally controlled clean conventional rooms supplied with high-efficiency particulate air under a 12-hour light to 12-hour dark cycle in an authorized animal facility of the Laboratory Animal Research Center at the National Institute of Radiological Sciences. Mice were monitored weekly for maintenance of body weight, and their health status was assessed twice daily [4]. All equipment and supplies, including cages, water bottles, and wooden chips used for bedding, were sterilized.

Diets

Diets of different caloric contents, 3.31, 3.35, 3.38, 3.42, and 3.48 kcal/g, were used. Caloric intake was adjusted by varying amounts of carbohydrate and dextrose, while providing constant amounts of other nutrients, such as proteins, lipids, vitamins, and minerals (Fig. 1). Noncaloric restricted (control) mice were provided 95 kcal/week, per mouse, based on the 3.48 kcal/g diet. For CalR, according to the body weight monitored three times a week, diets were of different calorie-controlled regimens, i.e., 60, 65, 70, 75, and 95 kcal/week, per mouse (see section, Calorie Restriction Procedure).

Irradiation

Mice were exposed to 3-Gy whole-body x-ray irradiation at a 200-kV/20-mA pulse using a therapeutic x-ray irradiator (Simadzu, Kyoto, Japan) with 0.5-mm Al and 0.5-mm Cu filters, at a dose rate of 0.614 Gy/minute and a 56-cm focus surface distance. All mice in the treatment group were irradiated at 10 weeks old.

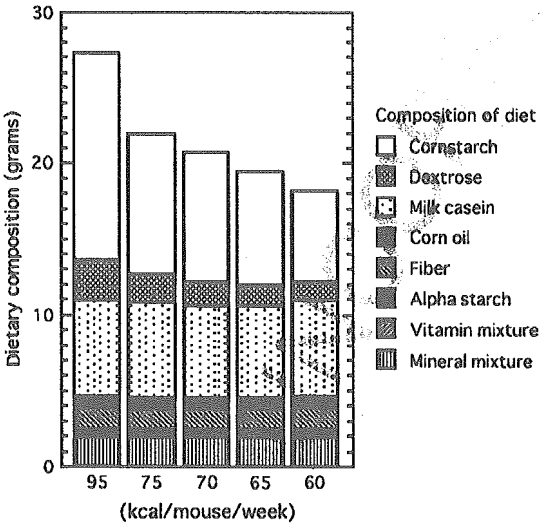

Figure 1. Five dietary regimens based on diets of different caloric contents (see text). The total, in grams, fed to each mouse per week is indicated in the bar graph for each dietary regimen. For caloric restriction, 60-, 65-, 70-, 75-, and 95-kcal dietary regimens, were used to maintain the body weight of each mouse within 25–27 g.

Calorie restriction procedure

Mice were subjected to four dietary conditions on the basis of the timing of CalR and thus divided into four groups: i.e., no restriction, CalR(–); preirradiation restriction (6–10 weeks old), CalR(pre); postirradiation restriction (from 10 weeks old to death), CalR(post); and a group subjected to lifetime CalR [from 6 weeks old to death, CalR(through)]. All of these groups were subdivided into two groups at 10 weeks old: those receiving 3-Gy irradiation or no irradiation (3 or 0Gy-) (see Irradiation section). Namely, there were eight groups; 3Gy-CalR(–) and 0Gy-CalR(–) groups, 3Gy-CalR(pre), and 0Gy-CalR(pre) groups, 3Gy-CalR(post) and 0Gy-CalR(post) groups, and 3Gy-CalR(through) and 0Gy-CalR (through) groups. The number of animals in each group is shown in Table 1. Identically designed cohort studies were combined; thus, animal numbers shown in Table 1 are different among the experimental groups.

Noncaloric restricted groups were fed a 95-kcal diet from 6 weeks old until death. Mice in the CalR(pre) groups were fed a 65-kcal diet from the start of the experiment, i.e., from 6 to 10 weeks old; thereafter they were fed a 95-kcal diet. Mice in the CalR(post) groups were fed a 95-kcal diet for the first 4 weeks old, i.e., from 6 to 10 weeks old, after which their body weights were controlled between 25 and 27 g with a 60- to 95-kcal dietary regimen. Caloric intake of the CalR(post) groups, however, exceeded their body weight by about 2 g, thus, it was fixed at 65 kcal from 10 to 12 weeks old until body weight decreased to 25 to 27 g. Mice in the CalR(through) groups were fed a 65-kcal diet for the first 4 weeks, i.e., from 6 to 10 weeks old, after which their body weights were controlled throughout their lifetime from 25 to 27 g with a 60- t- 95-kcal dietary regimen. Average caloric intake from 10 weeks old calculated was 77 kcal/week, per mouse, in the CalR(post) and the CalR(through) groups.

As in our previous study, all mice were observed throughout their lifespan. All mice—except for 8% that succumbed to leukemic sudden death—exhibiting or developing anemia, or having palpable spleens, were sacrificed during the agonal period. All sacrificed mice were confirmed to have been myelogenous and had been transplantable by transplantation assay [3]. This leukemogenicity was maintained also in p53-deficient C3H/He mice as determined by fluorescein-activated cell sorting, using c-kit, Mac-1, Gr-1, B220, sIgM, Thy1.2, and CD3, among others [10]. Conventional histological examinations were routinely performed at our laboratory [11,12]. Complete necropsies were performed and organs were examined both grossly and histologically. Tissues were fixed with 4% formaldehyde in phosphate-buffered saline, embedded in paraffin, sectioned at 4-μm thickness, and routinely stained with hematoxylin and eosin. Cause of death was identified in each case. Hepatomas observed in the present study have been described elsewhere [13].

Assay of HPCs

To monitor the number of HPCs, the number of progenitor cells per spleen and that per bone marrow were evaluated by in vivo and/or in vitro colonization assay at 10 and 14 weeks (see section, Calorie Restriction Procedure). Day-12 CFU-S were assayed by spleen colonization assay in accordance with the method of Till and McCulloch [14]. Mice irradiated with a lethal dose were injected intravenously with bone marrow cells or spleen cells from donor mice. Three femurs or three spleens from three donor mice of each group were pooled and assayed. Recipient mice

Table 1. ■

Experimental groups	No. of mice[a]	Median survival time in days[b] (range)	Myeloid leukemia		Other tumor		Tumor- free mice	
			No. of case	(%)[c]	No. of case	(%)[d]	No. of case	(%)[c]
0Gy-CalR(–)	258	839 (805–865)	3	1.2	299	115.9	26	10.1[g,h]
3Gy-CalR(–)	270	697 (678–730)	60	22.2[e,f]	308	114.1	20	7.4[i,j]
0Gy-CalR(pre)	93	885 (846–924)	2	2.2	111	119.4	10	10.8
3Gy-CalR(pre)	98	722 (679–772)	16	16.3	119	121.4	7	7.1
0Gy-CalR(post)	263	896 (874–925)	0	0	213	81.0	94	35.7[g]
3Gy-CalR(post)	274	805 (768–833)	26	9.5[e]	315	115.0	48	17.5[i]
0Gy-CalR(through)	69	874 (798–898)	0	0	40	71.0	32	46.4[h]
3Gy-CalR(through)	75	731 (690–845)	6	8.0[f]	76	101.3	15	20.0[j]

[a]No. of mice refers to number of effective mice. Accidental deaths occurred due to the leakage of water bottles; 5 in 0Gy-CalR(–), 1 in 0Gy-CalR(pre), 2 in 3Gy-CalR(pre), 4 in 0Gy-CalR(post), and 8 in 3Gy-CalR(post).
[b]Median survival time and the upper and lower 95% probability ranges estimated by the Kaplan-Meier method [17] (see Materials and Methods).
[c]Fisher exact test for the incidence of myeloid leukemia and tumor-free mice was performed.
[d]Percentages > 100% are due to multiplicity of tumor incidences.
[e]3Gy-CalR(–) vs 3Gy-CalR(post) ($p<0.0001$).
[f]3Gy-CalR(–) vs 3Gy-CalR(thru) ($p<0.01$).
[g]0Gy-CalR(–) vs 0Gy-CalR(post) ($p<0.001$).
[h]0Gy-CalR(–) vs 0Gy-CalR(thru) ($p<0.0001$).
[i]3Gy-CalR(–) vs 3Gy-CalR(post) ($p<0.001$).
[j]3Gy-CalR(–) vs 3Gy-CalR(thru) ($p<0.01$).

were sacrificed on day 12 (day-12 CFU-S) after cell transfusion. Spleens with or without colonies were fixed with Bouin's solution, and surface colonies were counted.

CFU-GM were also assayed by the methylcellulose method in semisolid culture [15]. Bone marrow cells and spleen cells were cultured in alpha medium supplemented with 20% fetal bovine serum and pokeweed-mitogen–stimulated spleen-cell–conditioned medium [15]. After 7-day incubation, all CFU-GM containing more than 50 cells were enumerated.

Assay of stem cell kinetics

The bromodeoxyuridine ultraviolet (BUUV) method was used, so designated on the basis of the incorporation of bromodeoxyuridine (BrdUrd) using an osmotic minipump, followed by the specific purging of BrdUrd-incorporated cells by exposure to ultraviolet light (UV) with a peak at 365 nm (UVA), and then followed by assaying the ratio of the number of hematopoietic colonies (CFU-S, in the present study) of the purged group to that of the control group. The CFU-S–specific parameters for cell kinetics, such as doubling time, size of cell cycling (undergoing DNA synthesis) or quiescent fractions, and also size of cell-cycling fraction during a unit time interval [16] were determined. Three mice each from the 0Gy-CalR(–) and CalR groups were examined at 50 weeks old, i.e., 44 weeks after caloric restriction for the CalR groups and generally close to the time that leukemogenesis is about to become overt.

Statistical analyses

Data were stored in a computer and processed for statistical analyses using the Kaplan-Meier method for survival curves and the log-rank test [17] for statistical significance. Median survival period and the upper and lower 95% probability ranges were calculated (Table 1). Incidences of hematopoietic malignancies and tumor-free death were evaluated by Fisher's exact test (Table 1).

Results

Effect of CalR diets on growth curves and survival

Body-weight changes in the experimental groups obtained in the present study are shown in Figure 2. There was no apparent difference in weight between unirradiated and irradiated mice in the same dietary group.

Body weights of the CalR groups given a 65-kcal diet for 6 to 10 weeks decreased to a mean weight of 22 g. Mice in these groups had lower body weights than those in the other experimental groups. Moreover, animals assigned to undergo a dietary regimen designed to maintain their weight

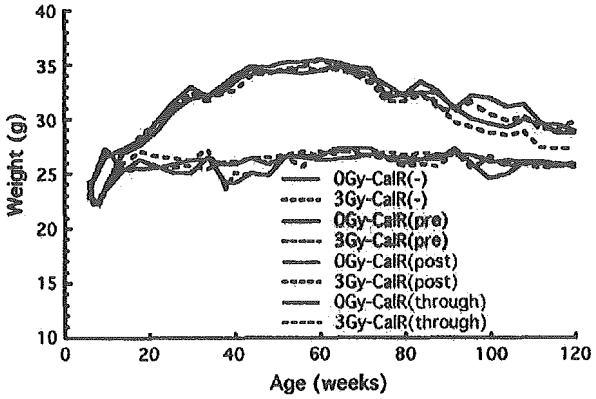

Figure 2. Changes in mean body weight vs age in weeks for all experimental groups, CalR(–), black; CalR(pre), red; CalR(post), green; and CalR(through), blue; with or without 3-Gy irradiation. Note the body weights of the 0Gy-CalR(pre) and 3Gy-CalR(pre) groups immediately returned to the non-CalR level after the dietary change at 10 weeks old, and their body weight profiles are similar to those of the controls, that is, the 0Gy-CalR(–) and 3Gy-CalR(–) groups (see text).

print & web 4C/FPO

between 25 and 27 g successfully after they reached 10 weeks old; indeed, achieved weights in this range. Changes in the body weight of the groups without caloric restriction are shown in Figure 2.

Survival curves for 3-Gy–irradiated groups with and without caloric restriction, and the 0Gy-CalR(–)group as a control are shown in Figure 3, and the comparable median survival periods (days) are listed in Table 1. Irrespective of the dietary regimen, there was a significant decrease in the lifespan of mice in all 3-Gy–irradiated groups compared with the 0-Gy groups (see, significances in legend to Fig. 3), and also in the median survival periods of mice in the 3-Gy–irradiated groups compared with the nonirradiated 0-Gy groups (697–805 days vs 839–896 days, in Table 1). Irrespective of dietary regimen, there was a significant difference in longevity among all the irradiated groups, except for the 3Gy-CalR(pre) group, compared with that of the irradiated group without caloric restriction.

CalR prevents radiation-induced myeloid leukemias

All four irradiated groups [3Gy-CalR(–), 3Gy-CalR(pre), 3Gy-CalR(post), and 3Gy-CalR(through)] demonstrated increased incidences of myeloid leukemias as compared with the corresponding nonirradiated groups [0Gy-CalR(–), 0Gy-CalR(pre), 0Gy-CalR(post) and 0Gy-CalR(through]; 1.2% to 22.2% ; 2.2% to 16.3%; 0.0% to 9.5%; and 0.0% to 8.0%, respectively) (Table 1).

As shown in Figure 4, onset of radiation-induced myeloid leukemias was markedly delayed by CalR, specifically in the 3Gy-CalR(through) group. Total incidence of myeloid leukemias in the 3Gy-CalR(through) group was the lowest ($p < 0.01$; Fisher's exact test). The increased rate of incidence and the total incidence of radiation-induced

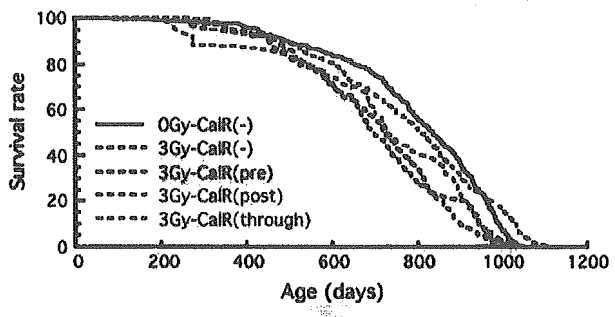

Figure 3. Survival curves for irradiated groups compared with nonirradiated control group; namely, the 3Gy-CalR(pre), 3Gy-CalR(post), and 3Gy-CalR(through) groups indicated by red, green, and blue dotted lines, respectively, are shown with those of the CalR(–) groups with or without irradiation; namely, the 3Gy-CalR(–) group indicated by a black dotted line and the 0Gy-CalR(–) group by a black solid line. For survival data for CalR groups, refer to Experimental Procedure section and Materials and Methods section. Note that the groups fed the calorie-restricted diet after 10 weeks of age without irradiation exhibit prolonged longevity. Log-rank test for mean survival curves; 3Gy-CalR(–) vs 3Gy-CalR(post) ($p < 0.0001$), 3Gy-CalR(–) vs 3Gy-CalR(through) ($p < 0.03$), 0Gy-CalR(–) vs 3Gy-CalR(–) ($p < 0.0001$).

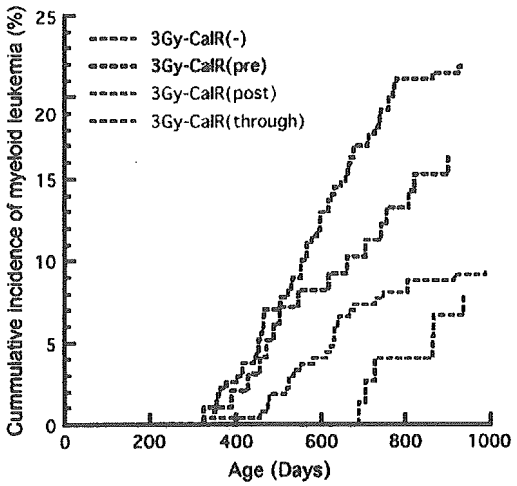

Figure 4. Cumulative incidence of myeloid leukemias. Incidences of myeloid leukemias in all the groups with caloric restriction, 3Gy-CalR(post), 3Gy-CalR(through) and 3Gy-CalR(pre) are lower than that in 3Gy-CalR(–) (see Table 1). The 3Gy-CalR(through) group shows the lowest incidence, whereas the 3Gy-CalR(post) group shows the second lowest. The 3Gy-CalR(pre) group shows a lower incidence than the 3Gy-CalR(–) group but with no statistical significance. The latency periods of the myeloid leukemias in the 3Gy-CalR(post) and 3Gy-CalR(through) groups were significantly prolonged as compared with that in the 3Gy-CalR(–) group.

leukemias in the 3Gy-CalR(post) group were lower than for those in the 3Gy-CalR(–) group (Fig. 4, $p < 0.0001$, Kaplan-Meier method; Table 1, 9.5% vs 22.2%; $p < 0.0001$, by Fisher's exact test). In the 3Gy-CalR(pre) group, neither onset delay, nor a significant decrease in the incidence of myeloid leukemias was observed, as compared with the 3Gy-CalR(–) group (Fig. 4, 325 days vs 321 days; Table 1; 16.3% vs 22.2%, resp.; $p = 0.217$, Fisher's exact test). However, there was no significant difference in the incidence of leukemia among the three caloric restriction groups, 3Gy-CalR(pre), namely, 3Gy-CalR(post), and 3Gy-CalR(though). When the changes in the incidence of myeloid leukemias for all of the CalR groups, except that for the 3Gy-CalR(pre) group, were examined, the increase in the incidence of myeloid leukemias noted in 3Gy-CalR (–) was prevented markedly. [Q4]

Because our primary aim was to examine radiation-induced myeloid leukemias and because we used strain C3H/He, a less-inducible strain for thymic lymphomas and lymphoid leukemias, hematopoietic neoplasms other than myeloid leukemias were not focused on in our examinations. Results show that there was no significant decrease in incidence due to CalR in any of the irradiated groups except for the nonirradiated groups, namely, the [Q5] 0Gy-CalR(post) and 0Gy-CalR(through) groups (data not shown).

Total incidence of nonhematopoietic neoplasms showed a limited decrease in only the 0Gy groups, i.e., the 0Gy-CalR(post) (81.0%) and 0Gy-CalR(through) groups (71.0%) as compared with 115.9% in the 0Gy-CalR(–)

print & web 4C/FPO

group (see Table 1 section, Other Tumors). These neoplasms include hepatomas/hepatocellular carcinomas, pulmonary tumors, tumors in the alimentary tract, genitourinary tumors, endocrine tumors, soft-tissue tumors, and dermal and skin-appendage tumors, among others.

Changes in number of hematopoietic stem/progenitor cells during or after caloric restriction

Because hemopoietic stem cells are assumed to be possible targets for radiation-induced leukemogenesis, and the number of hemopoietic stem/progenitor cells correlates proportionally to the number of CFU in vivo (CFU-S) and/or in vitro (CFU-GM), the numbers of CFU-S and CFU-GM were evaluated. A previous preliminary evaluation revealed that the number of hematopoietic stem/progenitor cells in the CalR groups decreases at the time of irradiation (10 weeks old) compared with that in the CalR(–) groups [9]. In this study, the number of HPCs at the time of irradiation (10 weeks old) and that 4 weeks after the dietary change (14 weeks old) were solely focused on and compared with those in the bone marrow and spleen (Fig. 5).

The 0Gy-CalR mice were fed a 65-kcal diet between the 6th week and 10th week. Thereafter, the 0Gy-CalR(pre) group was fed a 95-kcal diet, whereas the other 0Gy-CalR (through) group was fed the 65-kcal diet continuously. At 10 weeks old, as shown in Figure 5A (top left), the number of spleen cells in the CalR group markedly decreased as compared with that in the 0Gy-CalR(–) control group (1.32×10^8 vs 2.17×10^8 cells per spleen, respectively, second from the left vs far left). Although at 14 weeks old, in another CalR group, 0Gy-CalR(pre), the number of spleen cells originally assumed to be the same as that in the 0Gy-CalR(through) group did not decrease but rather increased as compared with the 0Gy-CalR(through) group (1.13×10^8 and 0.97×10^8 cells per spleen, respectively) due to the dietary change from a 65-kcal to a 95-kcal dietary regimen from 10 weeks old until 14 weeks old. In the 0Gy-CalR(post) group, CalR was not implemented until the 10th week; thereafter, in this particular experiment, the group was fed a 65-kcal diet until the 14th week. The number of splenic cells in the 0Gy-CalR(post) group had already significantly decreased by 14 weeks old, i.e., 4 weeks after the dietary change, as compared with the 0Gy-CalR(–) group (1.17×10^8 vs 2.00×10^8 cells per spleen).

In Figure 5B (middle, left), the numbers of progenitor cells (CFU-GM and day-12 CFU-S) per unit number of spleen cells are shown (from left to right). The number of colonies in vitro (CFU-GM) per 10^6 spleen cells for the 0Gy-CalR group markedly decreased as compared with that for the 0Gy-CalR(–) control group at 10 weeks old [lighter columns; $30.0/10^6$ cells for the 0Gy-CalR group, second from the left vs $191.7/10^6$ cells for the 0Gy-CalR(–) group, farthest left]. At 14 weeks old, the number of CFU-GM for the corresponding group, i.e., the 0Gy-CalR(through) group, showed a similar significant decrease as compared with the 0Gy-CalR(–) control group ($43.3/10^6$ cells vs $201.7/10^6$ cells). The 0Gy-CalR(pre) groups, whose number of CFU-GM was similarly assumed to be the same as that for the 0Gy-CalR(through) group, did not show any decrease as compared with the 0Gy-CalR(through) group ($136.7/10^6$ cells, $43.3/10^6$ cells, respectively) due to the dietary change from a 65-kcal to a 95-kcal dietary regimen from 10 weeks old to 14 weeks old. For the 0Gy-CalR(post) group, the number of CFU-GM significantly decreased as compared with the 0Gy-CalR(–) group ($46.7/10^6$ vs. $201.7/10^6$ cells) due to caloric restriction that started from 10 weeks old. Dday-12 CFU-S (Fig. 5B, darker columns; second column of each group) also showed a trend similar to that of CFU-GM. Thus, the numbers of progenitor cells per spleen, calculated from these values, are shown in Figure 5C (bottom; CFU-GM in lighter columns and day-12 CFU-S in darker columns). When Figure 5C is compared with Figure 5B, all values in the figure show a similar trend but are markedly higher than those shown in Figure 5B.

The number of HPCs in each group seems to correlate with the incidence of leukemia in each group. This may be due to differences in the numbers of stem/progenitor cells between the 0Gy-CalR(–) vs 0Gy-CalR(post) groups and between the 0Gy-CalR(through) vs 0Gy-CalR(pre) groups, induced by the dietary change at 10 weeks old and its subsequent consequences. For the readers' reference, three sets of data (Fig. 5D–F) comparable to those shown in Figure 5A to C but obtained from the bone marrow are presented. None of the data for groups for the bone [Q6] marrow showed any significant differences among the [Q7] groups.

Changes in cell-cycling fraction of the hematopoietic stem/progenitor cells during or after caloric restriction

Effect of caloric restriction on the cell-cycle kinetics was evaluated by BUUV assay [16]. In Figure 6, the cycling fraction of hemopoietic stem/progenitor cells is represented by the percentage killing of CFU-S. In this assay, only cycling CFU-S that incorporated BrdUrd were specifically killed by UVA (365-nm peak wavelength), causing a decrease in total number of colonies assayed in the irradiated spleen. The assayed bone marrow cells, as well as spleen cells, showed a significant decrease in percentage killing in the groups subjected to caloric restriction compared with the groups not subjected to caloric restriction [46.0% in the 0Gy-CalR(–) group vs 26.0% in the 0Gy-CalR group for the bone marrow, and 31.4% in the 0Gy-CalR(–) group vs 17.7% in the 0Gy-CalR group for the spleen; at 50 weeks old]. Because the fraction that incorporated BrdUrd and was killed by UV exposure refers to that which shows a reversal of the quiescent fraction, dormant fraction; caloric restriction restored the number of stem/progenitor cells in

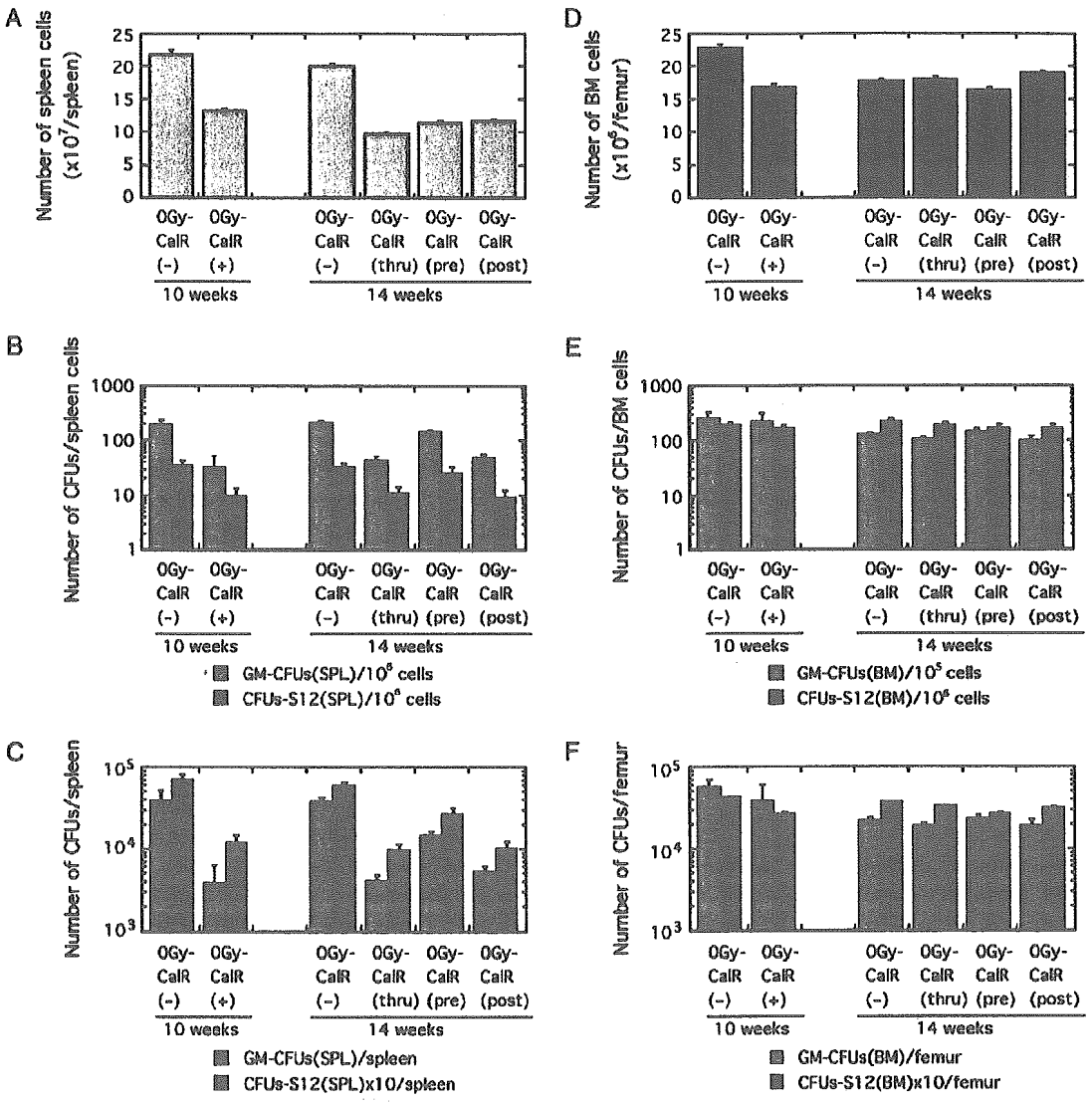

Figure 5. Number of hemopoietic cells (A,D), number of stem/progenitor cells per unit number of cells (B,E), and number of stem/progenitor cells per organ and/or tissue (C,F) are shown for the spleen (A–C) and femur (D–F). Each figure shows data at 10 weeks old, that is, 4 weeks after restriction started (left); and data at 14 weeks old, that is, 4 weeks after the dietary change (right). The right four columns represent the 0Gy-CalR(–), 0Gy-CalR(through), 0Gy-CalR(pre), and 0Gy-CalR(post) groups. For the two types of progenitor cell, the number of colony-forming units in the spleen (CFU-S) for day-12 (12D) granulocyte macrophage-colony-forming units (GM-CFU) determined by the in vitro assay was examined. Mice irradiated with a lethal dose of x-rays (810 cGy) were injected intravenously with spleen cells or femoral bone marrow cells from donor mice. For donor cells, three spleens or three femoral bone shafts from three donor mice of each group were pooled and assayed. Recipient mice were sacrificed on 12D (CFUs-S) after spleen cell transfusion. GM-CFU were assayed by methylcellulose method in semi-solid culture [15]. Spleen cells or femoral bone marrow cells were cultured in alpha medium supplemented with 20% fetal bovine serum and the pokeweed-mitogen-stimulated spleen-cell-conditioned medium (see Materials and Methods section in text). 0Gy-CalR(–) = mice fed a 95-kcal diet from 6 weeks old. CalR(thru) [CalR(through) in the text] = mice fed a 65-kcal diet from 6 weeks old. 0Gy-CalR(pre) = mice fed a 65-kcal diet from 6 to 10 weeks old, and thereafter a 95-kcal diet. 0Gy-CalR(post) = mice fed a 95-kcal diet from 6 to 10 weeks old, and thereafter a 75-kcal diet.

the quiescent state, which may also contribute to the prevention of leukemogenesis.

Tumor-free death with extension of lifespan by caloric restriction

On the basis of the observation that the percentage of mice that died free of any tumor increased significantly under the regimen of caloric restriction, the following question remains to be answered. Does suppression of tumor development contribute to changes in the spectrum of diseases other than tumors, and to the extension of lifespan, or to changes in the spectrum of disease attributable to tumor-free deaths?

The percentage of mice that died free of tumors was determined by anatomic and pathological examinations at